

The following manuscript is a non-peer reviewed preprint submitted to EarthArXiv on February 24th, 2023, and which will be submitted to 'Estuaries and Coasts'.

5 **Extrapolation based regionalized re-evaluation of the global estuarine surface area**

Goulven G. Laruelle¹, Judith A. Rosentreter^{2,3,4}, Pierre Regnier¹

¹ Dept. - Geoscience, Environment & Society (DGES)-BGEOSYS, Université Libre de Bruxelles, 1050 Bruxelles, Belgium

² Yale Institute for Biospheric Studies, Yale University, New Haven, USA

10 ³ Yale School of the Environment, Yale University, New Haven, USA

⁴ Centre for Coastal Biogeochemistry, Faculty of Science and Engineering, Southern Cross University, Lismore, Australia

Correspondence to: Goulven G. Laruelle (goulven.gildas.laruelle@ulb.be)

Abstract

15 At the interface between the continental and oceanic domains, estuaries are essential components of the land-ocean aquatic continuum that play a significant role in biogeochemical cycles, as they transform and export large amounts of carbon and nutrients from rivers to coastal waters. Because of this intense biogeochemical processing, they are significant ecosystems in terms of greenhouse gas exchange with the atmosphere. However, in spite of recent advances in remote sensing and the need for accurate estimates to calculate regional and global estuarine
20 budgets, the quantification of their global surface area has not been updated in over a decade and remains poorly constrained. This is due to the lack of a global extensive database, the diversity of estuaries, and the controversial definition of their boundaries. To address these challenges, a hybrid approach was developed that combines the surface areas of over 700 estuaries worldwide (extracted from the literature or calculated using geographic information systems) with a novel extrapolation method to provide type-specific regional estimates for 45 regions.
25 The upscaling formula applied is determined and calibrated using data from several regions where an extensive survey of total estuarine surface areas was available. The new global estimate of $733,801 \pm 39,892 \text{ km}^2$ is 31% lower than the previous global assessment and provides quantitative uncertainty estimates for regional and global estuarine surface areas as well as a breakdown between tidal systems and deltas ($294,956 \pm 30,780 \text{ km}^2$), lagoons ($179,946 \pm 12,056 \text{ km}^2$), and fjords ($259,899 \pm 22,328 \text{ km}^2$).

30 **Keywords**

Estuaries, surface area, biogeochemical budgets, typology, upscaling

1 Introduction

35 Estuaries can broadly be defined as aquatic transition systems at the interface between continents and oceans where freshwater mixes with marine water (Schwartz, 2005; Pritchard, 1967; Elliott and McLusky, 2002; Crossland et al., 2005). As such, they connect the terrestrial, riverine, marine, and atmospheric biogeochemical cycles, making them a critical component of the Land Ocean Aquatic Continuum (LOAC) which has been the centre of a growing interest in recent years (Billen et al., 1991; Cole et al., 2007; Cai, 2011; Regnier et al., 2013a, 40 2022; Bauer et al., 2020). Estuaries are dynamic biochemical ecosystems where both extensive primary production (Cloern et al., 2014; Woodland et al., 2015) and heterotrophic respiration take place (Bauer et al., 2013; Battin et al., 2022). The complex interplay between physical, biological, and chemical processes in estuaries (e.g. Vanderborcht et al., 2002; Volta et al., 2016; Regnier et al., 2013b) profoundly modifies the carbon and nutrient riverine loads before their export to the continental shelves and, ultimately the open ocean (Gattuso et al., 1998; 45 Mackenzie et al., 1998; Mantoura et al., 1991). For example, they exchange significant amounts of greenhouse gases (GHGs) such as CO₂, CH₄ and N₂O with the atmosphere (Borges 2005; Borges et al., 2005; Chen et al., 2013; Laruelle et al., 2013; Wells et al., 2018) and on longer time scales they can sequester large amounts of nutrients and carbon in their sediment (Nixon et al., 1995, Laruelle, 2009; Smith et al., 2015; Bianchi et al., 2020; Regnier et al., 2022). Therefore, estuaries play a significant role in global biogeochemical cycles, as recognized 50 in the latest global GHG budgets initiated by the Global Carbon Project (Friedlingstein et al., 2022; Tian et al., 2020; Saunio et al., 2020). Estuaries also host essential economical resources (Berbier et al., 2011), a unique biodiversity (Kennish, 2002; Filho et al., 2022), and provide opportunities for coastal development. For instance, 14 out of 20 of the largest cities in the world are located near the mouth of a river and the worldwide economic worth of aquaculture production in 2018 (including aquatic plants and inland water production) was estimated at 55 263 billion USD (Bartley, 2022), a large fraction of which is farmed in estuaries. Despite this strategic economic and scientific relevance, the only currently available estimates for global estuarine surface area are still poorly constrained, regionalized at a coarse spatial resolution, and has not been updated in over a decade (Dürr et al., 2011). Such lack of update may be surprising considering the recent improvement of remote sensing imagery and Geographic Information Systems (GIS), which in recent years have helped better constrain the spatial distribution 60 of other coastal ecosystems such as mangrove forests (Bunting et al., 2022), tidal marshes (Tootchi et al., 2019), and intertidal mud flats (Murray et al. 2018). This knowledge gap translates into an incompressible source of uncertainty in global biogeochemical estuarine budgets, effectively hampering upscaling efforts.

The first published estimate of the global estuarine surface area dates back to 1973, when Woodwell et al. (1973) extrapolated a ratio of estuarine surface area per length of coastline (the ‘Woodwell ratio’) from a 65 United States-based survey to the entire global coastline. For several decades, the resulting global estimate of 1.4 x 10⁶ km² was the only available figure and was thus widely used to extrapolate GHG emissions from estuaries from local to global scales (Abril and Borges, 2004; Borges, 2005; Borges et al., 2005; Chen and Borges, 2009; Frankignoulle et al, 1998; Jiang et al., 2008; Soetaert and Kroeze, 1998). The same surface area estimate was also used to constrain the size of the estuarine compartment of several global box models (Mackenzie et al., 1993, 70 1998, 2012; Ver, 1998; Ver et al., 1999; Rabouille et al., 2001, Laruelle et al., 2009) which have been used to investigate issues as diverse as coastal anoxia, estuarine nutrient retention, GHG exchange between aquatic compartment and the atmosphere or the fate of carbon along its journey through the LOAC. Only in 2011 was this estimate revised by Dürr et al. (2011) using an approach similar to that of Woodwell (1973) but refined by the use

of type-specific ratios of estuarine surface area per length of coastline, which brought the estimate down to 1.067
75 x 10⁶ km². In addition to a global surface area reduction, this new estimate paved the way for a refined global
analysis of the estuarine biogeochemical dynamics, since the type-specific assessment segregated fjords, tidal
estuaries, small deltas and lagoons, which typically exhibit distinct biogeochemical behaviours because of, for
example, characteristic freshwater residence times spanning several orders of magnitude between estuary types
(Dürr et al., 2011). Although a significant improvement since Woodwell et al. (1973), the updated surface-area
80 remained poorly constrained because the so-call ‘Woodwell ratios’ were only calibrated on very limited sections
of the world (United States: Engle et al., 2007; United Kingdom: DEFRA, 2008; Australia: Digby et al., 1998;
and Sweden: SMHI, 2009) and these national databases already highlighted significant inter-regional spatial
variability. Furthermore, the spatial resolution of the estuarine typology (0.5 degree) used by Dürr et al. (2011) to
calculate the lengths of coastlines implicitly assumed that only one type of estuary can be found within stretches
85 of several tens of kms. This update nonetheless sparked a significant interest from the scientific community and
allowed for several important revisions of the GHG emissions from estuaries (Laruelle et al., 2010, 2013; Abril
and Borges, 2012, Cai, 2011; Chen et al., 2013; Bauer et al., 2013; Regnier et al., 2013a, 2022; Ciais et al., 2021).
The type-dependant residence times also calculated by Dürr et al. (2011) provided a reference for the first spatially
explicit global estuarine modelling studies (Maavara et al., 2018; Laruelle, 2009), which were previously limited
90 to local or regional assessments in well-surveyed regions (Regnier et al., 2013b; Laruelle et al. 2017, 2019, Volta
et al., 2016).

In an age where remote sensing and GIS capabilities are sharply expanding, high resolution global
databases derived from satellite imagery are regularly updated for many types of ecosystems (e.g. Allen and
Pavelsky, 2018; Santoro et al., 2021; Reinhert et al., 2022). However, several technical challenges including the
95 complex definition of estuaries themselves (Bianchi, 2013; Dürr et al., 2011; Elliot and McLusky, 2002), the
delineation of their boundaries (Pritchard, 1967, Savenije, 2002) and their variations over time (Jiang et al., 2021)
are still major hurdles to release such data product for estuarine surface areas at regional and global scales. On the
other hand, while a growing number of national and regional estuarine databases have been published since the
early 2000s (Alder, 2003; CDLEM, 2003), the vast majority of the global coastline remains scarcely monitored.
100 In addition, the determination of estuarine surface areas by algorithms able to extract geometric properties from
satellite imagery (Jung et al, 2021), although promising, is still far from an automated procedure able to identify
each estuary over a continuous large stretch of coast. This technical challenge, in conjunction with an estimated
global number of estuaries in the tens of thousands (Mc Sweeney et al., 2017), highlights the difficulty to reach a
global assessment in the foreseeable future despite a growing number of exhaustive regional censuses.

105 In this study, we use a hybrid method relying on GIS-derived calculations for a limited number of
individual systems combined with an extrapolation strategy to provide regionalized estimates of estuarine surface
areas distinguishing three estuarine types in 45 regions worldwide. Furthermore, our study identifies, within each
of these so-called MARCATS region (for MARGins and CATchments Segmentation, Laruelle et al., 2013), the
largest estuarine systems for each estuarine type and provides the first quantitative estimate of the uncertainty
110 over the calculated regional estuarine surface areas, which is essential for an accurate assessment of estuarine
GHG budgets (Regnier et al., 2022). In this, context, we also provide estuary-type specific surface area estimates
for each of the RECCAP 2 regions (for the second Regional Carbon Cycle Assessment and Processes) as described
in Ciais et al. (2022). Our revised surface area estimate and associated uncertainty have recently been used in a

new observation-based meta-analysis of estuarine GHG budgets, including CO₂, CH₄ and N₂O (Rosentreter et al.,
115 in review), highlighting that our revision has profound implications for our understanding of the role of estuaries
in global carbon and nitrogen cycles.

2 Methods

2.1 Estuarine definition and typology

An estuary can be described as a coastal water body where marine and fresh waters mix above ground
120 (Bianchi, 2013; Schwatz, 2005; Pritchard, 1967; Dürr et al., 2011). As such, they are characterized by numerous
chemical (e.g., salinity, nutrients) and physical (e.g., tidal amplitude and energy) gradients and can widely vary
in size and shape depending on their geological settings. A broad definition of the term estuary includes systems
as diverse as fjords, tidal embayments, deltas, alluvial estuaries, or lagoons. There is no consensus in the literature
regarding the exact definitions of upstream and downstream boundaries of estuaries and different limits may be
125 used by different authors. Following Dürr et al. (2011), we use a geographic based definition of the lower boundary
at the interface with the coastal ocean corresponding to a virtual extension of the coastline regardless of potential
low salinity extension of estuarine waters onto the continental shelf (McKee et al., 2004). Not only can the global
surface area of these so-called ‘riverine plumes’ amount to several million of km² (Kang et al., 2013) but their
spatial extent also varies over time with changing freshwater discharge, tidal amplitude, and wind-induced mixing.
130 Upstream, several criteria also exist to define the limit between estuarine and inland waters. The two most
commonly used are the limits of the salinity intrusion and the length of the tidal influence (Bianchi, 2013;
Pritchard, 1967), Which can extend several times further inland (Dürr et al., 2011; Savenije et al., 2012). The tidal
river, the area with almost no salinity (<0.5) but still under tidal influence, has a length that can be significant (up
to several times the length of the salt intrusion, Savenije, 2005), but its width is usually much narrower than in the
135 brackish region of the estuary thus minimizing its contribution to the total surface area of the estuarine system.
Moreover, many rivers are dammed before the natural end of the tidal influence or even the salinity intrusion, in
which case the dam itself becomes the upstream limit of an estuary (e.g. Seine river, Laruelle et al., 2019). In this
work, following Dürr et al. (2011), we exclude the tidal river as part of the estuary. This choice is partly motivated
by the fact that, in a context of providing surface area estimates to constrain biogeochemical budgets, the salinity
140 limit is commonly used in such exercises as the frontier between estuarine and riverine domains (Seitzinger et al.,
2005; Mayorga et al., 2010; Canadell et al., 2015). Furthermore, only the saline portion of estuaries display
markedly different physical and biogeochemical behaviours compared to that of rivers (Regnier et al., 2013b).

Inspired by the typology proposed by Dürr et al. (2011), we distinguish three major estuarine groups:

1) ‘tidal systems and deltas’ which includes all open tidal systems from alluvial estuaries to tidal bays
145 and rias as well as deltas of any size, thus combining types I, II and V of Dürr et al. (2011)’s typology;

2) ‘lagoons’, which include enclosed shallow estuarine systems with minimal tidal influence and
relatively long water residence times, corresponding to types III in the Dürr et al. (2011) typology; and

3) ‘fjords’, which include all fjords with typical U-shaped valleys created by glaciers as well as other
coastal glacial depressions such as fjärds, defined as type IV in Dürr et al. (2011).

150 The original typology proposed by Dürr and colleagues thus relied on a larger number of classes than in
our study. Here, we decided to merge small deltas (type I) and tidal systems (type II), because their distinction

sometimes proved difficult to establish as many deltas (even the smaller ones) are often under tidal influence (e.g. Mekong, Amazon, Ganges) while several stable tidal estuaries display multiple channels and branches (e.g. Pearl River estuary), a key feature of deltaic systems. Furthermore, Dürr et al. (2011) defined estuaries fed by very large rivers (Ericson et al., 2004) as a separate type devoid of internal filter, arguing that characteristic residence times of freshwater within the estuarine limits of such systems are very short and do not allow for significant biogeochemical processing of riverine material prior to its export onto the continental shelf. While this assertion is partly supported by observations (McKee et al., 2004), such consideration is not relevant for our analysis that solely focusses on the determination of surface areas. Therefore, we merge types I, II and V of Dürr et al. (2011)'s classification into a single class in our calculations.

2.2 Novel upscaling procedure

An autonomous algorithm able to systematically determine estuarine areas over a continuous stretch of coastline has not yet been developed. In addition, performing such a task manually by individually determining the limits of each system through GIS would be a daunting task and has only been implemented at the regional scale in rare extensively surveyed zones (Engle et al., 2007; Digby et al., 1998). As a substitute for estuarine surface areas derived from an elusive global database, we developed an empirical prediction method that allows extrapolating the total surface area of a region from a limited number of measured systems. Somewhat similar approaches have been developed using scaling laws for the surface area and density of lakes (Downing et al., 2006) and other water bodies (Sagar, 2007; Bhang et al., 2019). Using data extracted from several national databases with exhaustive coverage of estuaries (United States, Australia, New Zealand: Hume et al., 2016; South Korea: Jung et al., 2021; South Africa: Van Niekerk, et al., 2013), we observed that the cumulative surface area of estuaries ranked in decreasing order of size over a stretch of coast consistently fits against the number of estuaries within that stretch of coast by an equation of the form:

$$S = \frac{a \times N}{b + N}, \quad (1)$$

with S being the cumulative estuarine surface area (km^2), N the number of estuaries, and a (km^2) and b (unitless), calibration coefficients. This equation, which plot is characterized by an initial steep increase converging towards a plateau implies that, as N tends toward infinity, S tends toward a , which thus corresponds to the asymptotic total surface area of the region. This function was retained for its limited number of input and fitting parameters. Preliminary tests revealed that to be a robust predictor, the equation requires an exhaustive coverage of a stretch of coast long enough to ensure inclusion of at least thirty systems, generally corresponding to several hundreds of kilometres. In order to take advantage of the apparent generic nature of equation (1), our extrapolation strategy consisted in first identifying and characterizing the ten largest estuaries of a given region and then in fitting equation (1) on the basis of this limited dataset to calculate the theoretical total surface area of the region (calibration term a of equation 1). In order to comply with the constraints of the method regarding the size and number of estuaries within a stretch of coastline and to work with regions characterized by relatively homogeneous estuarine settings, we used the global MARCATS segmentation (Laruelle et al., 2013), which delineates the global coastline into 45 regions.

Within each MARCATS and for each estuary type, the determination of the surface areas of the 10 largest systems of each estuarine type was achieved through the inspection of national databases (Australia, New Zealand,

190 Mexico, United States, South Africa, South Korea...), regional surveys (FAO, UNESCO...), global databases (Sea
Around Us, 2003), or published studies dedicated to a single or several systems. When no information was
available from this literature search (24% of the systems), the surface areas were calculated individually using
GIS. These calculations were performed with the help of QGIS using the novel 30-meter resolution global
shoreline vector dataset (Sayre et al., 2018). Overall, a total of 735 individual estuary surface areas were gathered
195 or calculated, 247 extracted from various databases, 311 for the literature and 177 calculated. Those data were
then sorted and fitted using equation (1) to derive the regionalized estuarine surface area for each MARCATS and
each estuarine type. The calculations were performed using MATLAB using the function *nlinfit* to determine the
coefficients a and b in equation (1).

The goodness of fit of the model was evaluated using the Mean Squared Error (MSE) calculated by the
200 function *nlinfit* using the following formula:

$$MSE = \frac{\sum R^2}{N-p} \quad (2)$$

Where R are the residuals representing the mismatch between the observed and calculated values of S,
N is the number of systems for which a comparison can be performed between the model and the observations
(i.e. 10 whenever possible) and p the number of parameters of the fitting formula used (i.e. 2). The square root of
205 this MSE was then reported to the average cumulated surface area of the dataset to provide a Relative Root Mean
Square Error (RRMSE) expressed as percentage representing the relative deviation of the fitted model reported to
the observations used to perform the extrapolation (10 for most MARCATS regions).

2.3 Strategies to quantitatively constrain uncertainties

Two different sources of uncertainties are accounted for in our calculations. The first, Δ_M represents the
210 uncertainty associated with our interpolation method while the second, Δ_S corresponds to the propagation at
regional scale of the uncertainty related to the determination of the surface area of individual systems δ_{Si} . Both
 Δ_M and Δ_S are expressed in km² and can be summed quadratically to quantify the total uncertainty Δ_T and are
described in detail in the following.

In order to quantify the uncertainty attributed to the extrapolation method itself (Δ_M), the term δ_M , which
215 represents the relative uncertainty (in %) associated with our extrapolation method had to be evaluated. To this
end, our predictive equation was applied using the 5, 8 or 10 largest systems located in the few MARCATS for
which all estuaries (and thus the total regional surface area) were known thanks to the available databases and for
which at least 30 estuaries of a given type were identified within the MARCATS. Five regions matched the above
criteria for deltas and tidal systems: along the Pacific US coast (MARCATS 2), along the Atlantic US coast
220 (MARCATS 10) as well as along MARCATS 34, 35 (Australia) and 36 (New Zealand). Four had sufficient data
coverage for lagoons: along MARCATS 20 (Mediterranean Sea), 34, 35 (Australia) and 36 (New Zealand).
Unfortunately, no region matched our criteria for fjords. Based on this analysis, we found that the normalized
standard deviation around the actual regional surface areas were 26, 12 and 9% for extrapolations relying on the
5, 8 and 10 largest systems, respectively (Fig. 1). These percentages were then used as best estimate for δ_M , Δ_M
225 being simply the product of the appropriate δ_M (depending on the number of systems used to perform the
extrapolation) and the corresponding surface area.

Because uncertainties over estuarine surface areas have only seldom been reported in previous studies,
providing a value for δ_{Si} is somewhat speculative. This uncertainty encompasses several sources of potential errors

ranging from the technical limitations associated with the spatial resolution of the map or dataset itself, to the
 230 determination of the boundaries of the system or the use of inconsistent definition of estuarine limits over several
 systems. To constrain these multiple sources of potential uncertainties, type-specific values of δ_{Si} were obtained
 by assembling a database of well-studied estuaries for which the surface area had been calculated independently
 at least three times (including this study). For each estuary, the multiple surface area estimates were first
 235 normalized to the mean surface area for that given system. All normalized values extracted from our literature
 search were then aggregated by type (56 for deltas and tidal systems, 45 for lagoons and 11 for fjords) in order to
 analyse their distribution (Fig. 2). All resulting distributions were exactly centred around 1 (per design) and
 successfully tested for normality using a Kolmogorov and Smirnov test with a 95% significance threshold
 (Massey, 1951). Their standard deviations were then calculated and yielded the following type specific values for
 δ_{Si} : 15% for deltas and tidal systems, 8% for lagoons and 4% for fjords.

240 In order to propagate the uncertainties attributed to the surface areas of each individual system belonging
 to the same MARCATS, Monte Carlo simulations were performed in which the surface area of each system used
 to perform the spatial extrapolation was randomly recalculated assuming a normal distribution centred on the
 observed surface area and characterized by δ_{Si} as standard deviation. Attention was paid to resort the estuaries by
 decreasing surface area in case the random recalculation of the individual surface areas modified the original
 245 order. Each Monte Carlo simulation was performed using 200 iterations, which proved sufficient to converge to
 a consistent mean regional surface area estimate within <1% (test performed using 100 sets of Monte Carlo
 simulations for several regions). The mean regional surface area calculated by the Monte Carlo simulation was
 considered the reference value for subsequent calculations and the standard deviation around this value was used
 as Δ_S for the calculation of the total uncertainty.

250 Using the mean surface area generated by the Monte Carlo simulations, the total uncertainty for a given
 estuarine type and a given MARCATS region is obtained using the following formula, in which SA is the total
 extrapolated estuarine surface area (km²):

$$\Delta_T = \sqrt{\Delta_M^2 + \Delta_S^2} = \sqrt{(SA \times \delta_M)^2 + (\Delta_S)^2} \quad (3)$$

255 A different strategy had to be used for the few regions and estuarine types for which exhaustive surveys
 were available in the literature, circumventing the need to apply our extrapolation method. This was the case for
 the lagoons surrounding the Mediterranean Sea (MARCATS 20), and all estuarine types located in New Zealand
 (MARCATS 36) and Australia (MARCATS 33, 34, 35). None of the corresponding databases provided an
 estimate of the surface area uncertainty, whether for individual systems or cumulated over the entire region.
 260 Therefore, the overall uncertainty for these regions was estimated by assuming that the uncertainties
 corresponding to each system can be approximated by δ_{Si} and propagated quadratically to the entire region using
 the following formula:

$$\Delta_T = \Delta_S = SA \frac{\delta_{Si}}{\sqrt{n}} \quad (4)$$

265

where n is the number of systems of a given type within the region, δ_{Si} is the type specific uncertainty for the
 considered system and SA, the total surface area of the n estuaries located in the region. This implies that the
 calculated relative uncertainty will decrease as the number of involved systems increases and that the total

uncertainties in these regions is significantly lower than in other regions considering that there is no uncertainty
270 attributed to the extrapolation.

2.4 Regional aggregation

2.4.1 MARCATS segmentation

The MARCATS segmentation was designed by Laruelle et al. (2013) to provide a multi-layer global
segmentation relevant for both oceanic and terrestrial analysis and upscaling strategies. This approach was
275 designed to build upon the COSCAT segmentation (for Coastal Segmentation and related CATchments, Meybeck
et al., 2005), which is a global segmentation of terrestrial land masses aggregating watersheds into relatively
homogeneous terrestrial units in terms of climate and hydrology. The MARCATS segmentation defines larger
units also accounting for oceanic features such as large-scale coastal currents following the classification of
continental shelf seas published by Liu et al. (2010). This simultaneous consideration of oceanic and terrestrial
280 constrains on segmentation units that do not compromise the integrity of riverine watersheds makes the
MARCATS segmentation ideally suited for the study of the LOAC (Regnier al., 2013, 2022). Designed like a set
of Matryoshka dolls, the MARCATS segmentation includes 3 nested layers: the watershed, the COSCAT and the
MARCATS.

The smallest unit of the segmentation are the ~6200 half degree resolution watersheds defined by a
285 widely used global hydrological network (Seitzinger et al., 2005; Mayorga et al., 2010). At a larger scale,
COSCATS segments are groups of these watersheds constrained by similar environmental forcings (e.g., climate,
lithology, geology) and which boundaries are defined by geographically explicit features (e.g., mountains, straits).
There are 149 exorheic COSCAT units in the MARCATS segmentation including 5 for Antarctica, which were
not included in Meybeck et al. (2005). Endorheic regions, such as the watershed surrounding the Caspian Sea are
290 thus not included in this segmentation, which primary interest is the connection between land and ocean through
the hydrologic network. The largest units, MARACTS segments typically consist in the aggregation of 2 to 6
COSCAT units but some MARCATS (16, 24, 19, 33, 35), only contain a single COSCAT because of very specific
coastal features such as a relatively limited upwelling system. MARCATS 20 (the Mediterranean Sea) includes
as many as 9 COSCATs. The rationale for the grouping of COSCAT units into a MARCATS was mostly based
295 on the continental shelf classification of Liu et al. (2010) which identified Eastern and Western boundary currents
as well as Marginal Seas and Monsoon influenced coasts. The remaining continental shelves were distributed
among three additional classes based on climatology: polar, sub-polar and tropical.

2.4.2 RECCAP 2

An important motivation for this regionalized re-evaluation of the global estuarine surface area is to
300 provide a more reliable framework for global GHG budgets such as those previously performed by Borges and
Abril, 2011; Laruelle et al., 2010, 2013; Chen et al., 2013 and now by Rosentreter et al. (in review). Therefore,
our results were further aggregated at the continental scale using the global regionalization defined in the context
of the RECCAP 2 initiative. Introduced in 2012 during the RECCAP 1 initiative (Canadell et al., 2012), the
RECCAP segmentation has been increasingly used since then (e.g., Ciais et al., 2020) including in the recent
305 Global Carbon Project syntheses (Friedlingstein et al., 2022). Several versions of this segmentation have been
published since 2012 and the earliest releases used two different sets of regional segmentations for oceans and

continents. In the recent RECCAP 2 initiative, however, an effort similar to that of the MARCATS approach was made to design consistent regional limits between both continental land masses and oceans (Ciais et al., 2022). The ten resulting world regions are thus ideally designed to investigate systems such as estuaries, which are located at the interface between continents and oceans. The geographic limits of the RECCAP 2 regions and their names can be found in figure 3.

In order to provide estuarine surface areas for each RECCAP region, the surface areas of all MARCATS regions which coastline was entirely comprised within a RECCAP region were entirely allocated to the latter. For MARCATS for which coastlines were distributed over two or more RECCAP regions, the total estuarine surface area was distributed for each type on a pro rata basis following the surface area-weighted distribution of the ten largest estuarine systems within the MARCATS. For instance, MARCATS 8 (Caribbean Sea) extends through RECCAP regions 1 (North America) and 2 (South America). Six of the ten largest lagoons of MARCATS 8 are located within RECCAP region 1 for a cumulative surface area of 4476 km². This means that 24% of the total surface area of the ten largest lagoons of MARCATS 8 (i.e. 18,505 km²) is located within the geographical boundaries of RECCAP region 1 and, subsequently, 24% of the extrapolated surface area of lagoons for MARCATS 8 (19692 km²) were allocated to the lagoon surface area of RECCAP region 1. Similar calculations are used for each estuarine type and uncertainties and also propagated in the same fashion using quadratic sums. Using quadratic sums to propagate uncertainties among estuarine types and regions ensures that the global total uncertainties remain consistent when computed by adding the uncertainties of all RECCAP regions or MARCATS.

3 Results and discussion

3.1 Global distribution

Overall, our calculations yield an updated estimate for the global estuarine surface area of 733,801 ± 39,892 km². This total surface area is distributed relatively evenly between tidal systems and deltas (294,956 ± 30,780 km²), lagoons (179,946 ± 12,056 km²), and fjords (259,899 ± 22,328 km²) but represents a total downward revision of 291,777 km² compared to the most recent estimate of 1,067,198 km² by Dürr et al. (2011). This decrease is particularly pronounced for fjords (-43%) and less so for other systems (-18% for tidal systems and deltas and -29% for lagoons, respectively). The surface areas for each estuarine type and each MARCATS are listed in table 2, along with their confidence intervals. Note that all global type-specific estimates from Dürr et al. (2011) are well outside the confidence intervals calculated in our study. An estimation of the goodness of fit between the observed cumulative surface areas and those calculated using our extrapolation methods for the largest systems of each MARCATS is calculated using equation (2) and reveals a good match between calculated surface areas and observed ones (Fig. 4a). For all estuary-types, the relative errors between observed and calculated surface areas (RRMSE) mostly ranges between 1 and 4%, giving confidence to our extrapolation method. Lagoons are the estuarine types for which the relative errors are the largest with a median value across all MARCATS slightly larger than 3% but, other than 2 outliers (deltas and tidal systems in MARCATS 12 and lagoons in MARCATS 4), the relative error never exceeds 6% for any estuarine type in any other MARCATS. Also noteworthy is the relative contribution to the total regional surface area of the 10 largest systems within a given MARCATS (Fig 4b). This contribution can vary significantly between 60 and 95% but overall is large, highlighting the disproportionate contribution of the largest estuaries to the total surface area of any given region.

This proportion appears to be largest for tidal systems and deltas and smallest for fjords in our calculations. This could be a reflexion of the geomorphologically different origins of these systems. Indeed, the shape of deltas and estuaries is constrained by the dynamic interplay of tidal energy, sediment loads and riverine discharge (Savenije, 2005; Regnier et al., 2013b) while the shape of fjords is carved into rocks by glaciers over longer timescales (Syvitski, 1987; Bianchi et al., 2020). Our exhaustive survey of individual estuarine surface areas which includes 735 systems amounts to cumulated surface areas of 239,005 km², 117,195 km², 176,477 km², for tidal systems and deltas, lagoons and fjords respectively. These numbers, which correspond to the largest systems within each MARCATS, for which individual surface areas could be either found in the literature or calculated through GIS correspond to 81%, 65% and 68% of the global surface area estimated by our extrapolation method for tidal systems and deltas, lagoons, and fjords, respectively.

The global distribution of estuarine surface areas per MARCATS is reported in figure 5a using pie charts where the size is a function of the cumulative surface area of the considered MARCATS. This reveals very pronounced first order spatial patterns with, naturally, fjords distributed among 13 MARCATS only, all located at high latitudes in agreement with Bianchi et al. (2020). It is noteworthy that MARCATS 13, 14 and 15 (i.e. the Canadian Archipelagos and Greenland) account for more than 75% of the global total while the rest of the fjords are distributed among Northern Europe, Russia, New Zealand, and Chile. No clear latitudinal pattern appears to discriminate between the spatial distribution of tidal systems and deltas and of lagoons. However, strong regional contrasts exist. For instance, these estuarine types (tidal systems and deltas and of lagoons) located along the Pacific coast of North, Central and South America, where a watershed are relatively small, gather a cumulated surface area several times smaller than along the Atlantic coast, Arctic regions excluded. Similarly, the Indian coast of Africa hosts a smaller estuarine surface area than along the Atlantic coast, which is characterized by larger watersheds. These observations might have suggested the existence of a relationship between the surface areas of estuaries and the size of their watersheds. However, a linear regression reveals that, although statistically significant ($p < 0.05$), the trend at the MARCATS scale is weak ($r^2 = 0.11$) and not more significant than the relationships between estuarine surface area and length of the coastline ($r^2 = 0.12$) or between estuarine surface area and riverine discharge ($r^2 = 0.09$). The regional distribution of surface areas between all three types is generally consistent with the global estuarine typology of Dürr et al. (2011) reported in figure 5b. The most notable difference is the larger contribution of lagoons to the estuarine surface areas of Eastern Siberia and along the Pacific coast of China (MARCATS 41 and 43) in our study, while these systems only represent a relatively small fraction of the coastline. MARCATS where lagoons are largely represented in the typology of Dürr et al. (2011) do translate into large surface areas as can be seen around the Gulf of Mexico (MARCATS 9) and the Caribbean Sea (MARCATS 8) or along the Western coast of central Africa (MARCATS 24). Divergences between our calculations and the typology of Dürr et al. (2011) can result from the disproportionate contribution of single large systems (e.g. Lagos lagoon) along the Southern Brazilian coast (MARCATS 5) or in a MARCATS characterized by a relatively small total surface area (MARCATS 33).

3.2 RECCAP-scale aggregation and comparison with prior continental-scale estimate

Table 3 reports the global distribution of estuarine surface areas per estuary type and RECCAP region. For comparison, surface areas derived from Dürr et al. (2011) are also reported, allowing us to understand if the downward global revision is homogeneously distributed or if regional patterns emerge. Note that the values

385 recalculated after Dürr et al. (2011) for each RECCAP region involve minor rounding discrepancies which lead
to a slightly lower total global surface area estimate but the mismatch does not exceed 1%. In both our calculation
and that derived from Dürr et al. (2011), North America (RECCAP region 1) contributes the largest share of the
global estuarine surface area, with 59% (328,885 km²) and 41% (428,016 km²) in our study and Dürr et al. (2011),
respectively. This disproportionate contribution is largely due to Canada's and Greenland's fjords, which account
390 for >75% of the global surface area of these estuarine systems. Our updated total estuarine surface area for North
America is 23% smaller than that of Dürr et al., (2011) and the distribution among estuarine types also differs
with equal contributions of tidal systems and deltas and lagoons in our calculations while the surface area of
lagoons is almost twice as large as that of tidal systems and deltas in Dürr et al. (2011). South America (RECCAP
region 2) displays the second largest estuarine surface area in our study (111,266 km²) while it is only fourth
395 (79,027 km²) in Dürr et al., (2011). The respective distributions across types are similar in both studies. South
America and South Asia (RECCAP region 8) are the only regions for which our updated surface areas exceed
those calculated by Dürr et al. (2011). Europe's (RECCAP region 3) estuarine surface area is less than half in our
calculations than what was predicted by Dürr et al., (2011) with large downward revisions for tidal systems and
deltas as well as for fjords but similar surface areas in both studies for lagoons. Africa's (RECCAP region 4)
400 estuarine surface area decreased by a factor of two in our study (37,182 km²) compared to the estimate of 84,733
km² by Dürr et al. (2011). This reduction is mostly attributed to lagoons, which surface area was 46,052 km² in
Dürr et al., (2011) and is now only 14,688 km² according to our calculations. Note that the 10,229 km² of fjords
allocated to Africa in the calculation derived from Dürr et al., (2011) actually correspond to the Kerguelen Islands
which falls within the domain of RECCAP region 4 while being located in the Southern Ocean (see Fig. 1) and is
405 considered devoid of estuaries in our study. Russia (RECCAP region 5) is, after North and South America, the
third largest contributor to the global estuarine surface area in our estimate and the second following Dürr et al.
(2011). In the latter assessment, fjords dominated the estuarine surface area (33%) in the region while they only
contribute 20% in our calculations. Tidal systems and deltas (58%) account for the largest share (48% in Dürr et
al., 2011). West Asia (RECCAP region 6) estuarine surface area mostly corresponds to the coasts surrounding the
410 Arabic peninsula and displays, by far, the smallest estuarine surface areas with 2,465 km² in our study and 5,265
km² in Dürr et al. (2011). Tidal systems and deltas largely dominated the surface area estimate in Dürr et al., 2011
while in our calculations the distribution is almost evenly spread between tidal systems and deltas and lagoons.
East Asia (RECCAP region 7) is characterized by the second smallest estuarine surface area in our re-evaluation
(12,558 km²), a value that is much smaller than the 39,017 km² reported by Dürr et al. (2011) that resulted from
415 a significantly larger contribution of lagoons. South Asia (RECCAP region 8) estuarine surface area is largely
dominated by tidal systems and deltas in our study (80%) in contrast to Dürr et al. (2011) that identified lagoons
as the highest relative contributor in the region (54%) despite a slightly lower overall surface area in their study
(21,585 km²) compared to ours (28,171 km²). Southeast Asia (RECCAP region 9) is the region with the largest
discrepancy between both studies: 85,036 km² according to Dürr et al. (2011) and 22,420 km² in our calculations.
420 This large estimate in Dürr et al. (2011) results from the long coastlines of Indonesia and Philippines which do
not translate into a large estuarine surface area in our calculations because of the relatively modest size of the
systems found in the region. In both cases, however, these surface areas are largely dominated by tidal systems
and deltas (>80%). Finally, Australasia (RECCAP region 10) shows relatively similar estuarine surface areas in
our study (45,880 km²) and in Dürr et al. (2011)'s (51,600km²) but they are characterized by different distributions

425 among estuarine types which are largely dominated by tidal systems and deltas in Dürr et al. (2011) and more evenly distributed in our study.

Overall, our study thus suggest that the global estuarine surface area is more strongly evenly distributed at the continental scale than previously advocated. In spite of yielding a significantly different global estimate for the estuarine surface area, it is worth noting that our work does not contradict the typology of Dürr et al. (2011) in itself in terms if spatial distribution of estuarine types but highlights the limits of using consistent ratios to extrapolate estuarine surface areas from coastlines worldwide. Qualitatively, a relatively good qualitative match can be observed between our spatial distribution of the different estuarine types compared to Dürr et al. (2011). Both studies also make the same assumption that Antarctica is devoid estuaries because the vast majority of the Antarctic continent is covered by large ice sheets and does not present persistent aerial rivers able to form estuaries when they flow into the coastal ocean. The recent global study on fjords published by Bianchi et al. (2020) and the earlier work from Syvitski (1987) provide a qualitative global distribution of fjords worldwide that is consistent with the global distribution in our study. In their study, Bianchi et al. (2020) only consider a marginal occurrence of fjords in Antarctica at the tip of the Antarctic Peninsula.

3.3 Zooming on previously surveyed regions

440 Very few regional studies (which data are not included in our calculations) can be used to further evaluate our updated estimate. To our knowledge, only three studies addressing regions larger than a MARCATS unit have provided estimates of estuarine surface areas. The oldest one, from Quasim (1982), evaluated the total surface area of India to 27,000 km². Indian's coast covers MARCATS 31 and MARCATS 32, which cumulative estuarine surface area amounts to 31,717km² (84% for tidal systems and deltas and 16% for lagoons). This number is in reasonable agreement with Quasim (1982)'s estimate considering that MARCATS 32 not only include the Eastern coast of India but also that of Bangladesh which embraces the mega-delta of the Ganges-Brahmaputra rivers. In our calculation, the latter exceeds 10,000 km², a fraction of which flows into India through the branch of the delta fed by the Hoogly river. The surface area of all estuaries and lagoons of Mexico have been evaluated by Ortiz-Lozano et al. (2005) to 28,500 km² (16,000 for estuaries and 12,500 for lagoons). The coast of Mexico is mostly included in MARACTS 2 (on its Atlantic side), MARCATS 9 (flowing into the Gulf of Mexico) and marginally in MARCATS 8 (Caribbean Sea). The combined surface area of deltas and tidal estuaries of MARCATS 2 and 9 only amounts to 8,628 km² while the combined surface area of lagoons of MARCATS 2 and 9 exceeds 40,000 km². However, a significant fraction of these estuaries is located in the United States. Removing this contribution, the remaining total for the two estuarine types reaches circa 30,000km², which is comparable to Ortiz-Lozano et al. (2005) but with a very different distribution between tidal systems and deltas and lagoons. The comparison is difficult to carry further considering that little information is available on the calculations carried out by Ortiz-Lozano et al. (2005) or on their approach to segregate the two estuarine types.

Perhaps the most relevant comparison can be performed against the more recent publication by Upstill-Goddard and Barnes (2016), which evaluated the surface area of European estuaries to 34,000 km² by extrapolating a ratio of estuarine surface area per coastline length of the United Kingdom to the entire continent. Although the details of the calculation were not provided, this value excludes fjords and is comparable with our total of ~29,000 km² for tidal systems and deltas and lagoons in RECCAP region 1. The convergence between both estimates contrasts with the assessment of ~51,000 km² derived for the same systems and same region by

Dürr et al. (2011) and especially the older assessment of ~160,000 km² (likely including fjords) reported by Bange
465 (2006), as derived from a loose extrapolation from Woodwell et al. (1973). The work by Upstill-Goddard and
Barnes (2016) is particularly interesting because, compared to the estimates derived from Dürr et al. (2011) and
Bange (2006), it sheds light on how the use of ratios of estuarine surface area to coastline length at global scale
can lead to diverging results but can be a more reliable approach regionally, provided that the ratios are calculated
on a segment of coast located within the region as was done by Upstill-Goddard and Barnes (2016).

470

3.4. Uncertainties, limitations, and future work

While one of the motivations behind the recent revisions of the global spatial distributions and surface
area of many aquatic ecosystems often targets the reduction of uncertainty in their geographic extent, very few
475 studies actually attempt to quantify these uncertainties numerically. This is particularly true for estuaries. To our
knowledge, we provide the first global or regional estimation of estuarine surface areas that includes an explicit
quantification of the uncertainty. This lack of quantitative assessment in previous work can partly be explained
by the diversity of potential sources of uncertainties associated with the calculation of the surface area of an
estuarine system, let alone the challenge of upscaling such uncertainties at the regional scale. The very definition
480 of an estuary and its boundary can significantly vary among authors (Elliot and McLusky, 2003). Consequently,
there is no consensus regarding the number of estuaries worldwide. From the lower bound estimate of 4,464
proposed by Harris et al. (2016) loosely based on Dürr et al. (2011) to the more likely figure of 53,000 by Mc
Seeney et al. (2017) derived from GIS calculations using a global digital elevation model, the uncertainty exceeds
an order of magnitude. The fact that global high-resolution hydrographic networks such as Hydrosheds (Lehner
485 et al., 2008) connect ~60,000 watersheds to the ocean gives credence to Mc Seeney et al. (2017)'s estimate but
the actual number may be even larger because many small systems are still not resolved by such global
calculations and databases. Moreover, in large deltaic systems or complex semi-enclosed embayments fed by
several rivers, the entire system can either be considered a single estuary or be subdivided in as many estuaries as
there are many rivers. For instance, the Chesapeake Bay can be considered a single estuary or, based on its
490 numerous feeding rivers, could reach a value as high as several dozen.

A more quantifiable source of uncertainty relates to the definition of the upstream boundary of an
estuarine system. Assuming an exponential decrease of the estuarine width along its longitudinal axis governed
by its so-called convergence length (Savenije, 1986; 2005), we used the following equation to determine the
surface area of the saline and tidal estuaries for several systems for which sufficient data was available:

495
$$b_z = b_0 \cdot \exp\left(-\frac{z}{CL}\right) \quad (5)$$

In the equation above, b_z is the estuarine width at distance z (in km) from the mouth, b_0 is the estuarine
width at the mouth and CL is the convergence length of the estuary, which characterizes the shape of the system.
Using published data for 19 estuarine systems, for which the parameters required to apply equation (5) to the tidal
and saline estuary were available we calculated their respective surface areas (table 4). While the length of the
500 tidal intrusion generally exceeds that of the saline intrusion by a factor ranging from 1 to 5, the resulting difference
in surface area is generally much smaller and below 15% in the majority of the 19 systems investigated (12 systems
for which the ratio of the surface areas of the saline estuary over that of the tidal estuary exceeds 0.85, table 4). In

addition, it is interesting to note that the range of surface area differences is comparable to the uncertainty σ_{Si} of the surface area of individual deltas and tidal systems calculated in section 2.3.

505 While our extrapolation strategy is a significant advance from previous estimates (Woodwell et al., 1973; Dürr et al., 2011), the increasing number of recent high resolution, spatially explicit databases derived from remote sensing imagery and GIS applied in coastal wetlands (Tootchi et al., 2019; Bunting et al., 2022, Murray et al. 2018, 2022) suggests that, ultimately, a similar data product should become available for estuaries as well. Nevertheless, the complexity of defining estuaries and their boundaries still poses a challenge for large-scale
510 automation based on these technologies. In addition, approaches relying upon remote sensing imagery will have to face additional challenges that have not yet been resolved such as the changing nature of the connection of estuarine systems with adjacent coastal seas which would require a temporal acquisition. Indeed, in their global investigation of Intermittently Closed/Open Lakes and Lagoons (ICOLL), Mc Sweeney et al. (2017) evaluated that ~3% of coastal lagoons worldwide are not permanently connected to the sea throughout the year. In addition
515 to that number, how many temporary estuaries only exist after unusual precipitation events in arid regions (Arthington et al., 2014), especially under a future changing climate? As a promising avenue, a tool exploiting readily available spatialized dataset derived from remote sensing has recently been developed (Jiang et al., 2021). This MATLAB algorithm was successful applied manually to >100 estuaries surrounding South Korea and calculates the surface area as well as other geometric parameters such as the width at the mouth, the length and
520 the convergence length of a given estuary. It demonstrates that the algorithm can be applied to a continuous stretch of coast and diagnose a multitude of tidal estuaries, including very small ones. However, this algorithm will likely need to be modified if deltaic systems with multiple branches or complex lagoon geometries need to be recognised and processed with equal performance. Furthermore, considering the sheer number of estuaries worldwide (conservatively estimated in the tens of thousands by Mc Sweeney et al., 2017), the current lack of an automated
525 procedure remains a major limitation for large-scale applications. Our semi-empirical upscaling method, while still relying on a number of assumptions associated with diverse uncertainties, bridges the gap between a partly outdated estimate (Dürr et al., 2011) and the development of future global remote-sensing based databases that is still likely several years away.

5 Author contributions

530 GGL designed the study and performed all the calculations following several discussions with JAR and PR. All authors contributed to the manuscript after an initial draft from GGL.

6 Competing interests

The authors declare that they have no competing interests.

7 Acknowledgements

535 Goulven G. Laruelle is research associate of the F.R.S-FNRS at the Université Libre de Bruxelles and acknowledges funding by the nuts-STeauRY project funded by the French Office of Biodiversity (OFB). Judith A. Rosentreter acknowledges funding by the Yale Institute for Biospheric Studies at Yale University. Pierre Regnier received financial support from the European Union's Horizon 2020 research and innovation programme

under Grant Agreement no. 101003536 (ESM2025 – Earth System Models for the Future) and from BELSPO
540 through the project ReCAP, which is part of the Belgian research program FedTwin,

References

- Alder, J.: Putting the coast in the Sea Around Us Project, *The Sea Around Us Newsletter*, 15, 1-2, 2003.
- Abril, G. and Borges, A. V.: Carbon dioxide and methane emissions from estuaries, in: *Greenhouse Gases Emissions from Natural Environments and Hydroelectric Reservoirs: Fluxes and Processes*, edited by: Tremblay, A., Varfalvy, L., Roehm, C., and Garneau, M., Springer, Berlin, 187-207, 2004.
545
- Allen, G. H. and Pavelsky, T. M.: Global extent of rivers and streams, *Science*, 361(6402), 585-588, doi:10.1126/science.aat0636, 2018.
- Arthington, A. H., Bernardo, J. M. and Ilhéu, M.: Temporary rivers: linking ecohydrology, ecological quality and reconciliation ecology, *River Res. Applic.*, 30, 1209-1215, doi:10.1002/rra.2831, 2014.
- 550 Audry, S., Blanc, G., Schäfer, J., Guérin, F., Masson, M., and Robert, S.: Budgets of Mn, Cd and Cu in the macrotidal Gironde estuary (SW France), *Marine Chemistry*, 107, 433-448, 2007a.
- Barbier, E. B., Hacker, S. D., Kennedy, C., Koch, E. W., Stier, A. C., and Silliman, B. R.: The value of estuarine and coastal ecosystem services, *Ecological Monographs*, 81(2), 169-193. <https://doi.org/10.1890/10-1510.1>, 2011.
- 555 Barnes, J., and Upstill-Goddard, R. C.: N₂O seasonal distributions and air–sea exchange in UK estuaries: implications for the tropospheric N₂O source from European coastal waters, *J. Geophys. Res.*, 116, G01006, doi:10.1029/2009JG001156, 2011.
- Bartley, D. M.: *World Aquaculture 2020 – A brief overview*, FAO Fisheries and Aquaculture Circular No. 1233. Rome, FAO, <https://doi.org/10.4060/cb7669en>, 2022.
- 560 Bange, H. W.: Nitrous oxide and methane in European coastal waters, *Estuarine Coastal and Shelf Science*, 70, 361-374, doi:10.1016/j.ecss.2006.05.042, 2006.
- Bauer, J. E., Cai, W. J., Raymond, P. A., Bianchi, T. S., Hopkinson, C. S., and Regnier, P. A. G.: The changing carbon cycle of the coastal ocean, *Nature*, 504, 61-70, doi:10.1038/nature12857, 2013.
- Bhang, K. J., Schwartz, F. W., Lee, H. W., and Park, S. S.: Scaling effect of lake distribution on power law by coastal area simulation, in: *The 3rd International Water Safety Symposium*. edited by Lee, J. L., Yoon, J.-S., Cho, W. C., Muin, M., and Lee, J., *Journal of Coastal Research*, Special Issue No. 91, 301-305. Coconut Creek (Florida), ISSN 0749-0208.
- Bianchi, T. S.: Estuaries: Where the Rivers Meets the Sea, *Nature Education Knowledge*, 4(4),12, 2013.
- Bianchi, T. S., Arndt, S., Austin, W. E. N., Benn, D. I., Bertrand, S., Cui, X., Faust, J. C., Kozirowska-makuch, K., Moy, C. M., Savage, C., Smeaton, C., Smith, R. W., and Syvitski, J.: Earth-science reviews fjords as aquatic
570 critical zones (ACZs), *Earth Sci. Rev.* 203, 103-145, doi:10.1016/j.earscirev.2020.103145, 2020.
- Billen, G., Lancelot, C., and Meybeck, M.: N, P, and Si retention along the aquatic continuum from land to ocean, in: *Ocean margin processes in global change*, edited by: Mantoura, R. F. C., Martin, J. M., and Wollast, R., John Wiley and Sons, New York, 19-44, 1991.
- 575 Borges, A. V.: Do we have enough pieces of the jigsaw to integrate CO₂ fluxes in the coastal ocean?, *Estuaries*, 28, 3-27, 2005.

- Borges, A. V. and Abril, G.: Carbon dioxide and methane dynamics in estuaries, in: *Treatise on Estuarine and Coastal Science*, Vol. 5, edited by: Wolanski, E. and McLusky, D. S., 119-161, Academic Press, 2012.
- Borges, A. V., Delille, B., and Frankignoulle, M.: Budgeting sinks and sources of CO₂ in the coastal ocean: diversity of ecosystems counts, *Geophys. Res. Lett.*, 32, L14601, doi:10.1029/2005GL023053, 2005.
- 580 Bunting, P., Rosenqvist, A., Hilarides, L., Lucas, R.M., Thomas, T., Tadono, T., Worthington, T.A., Spalding, M., Murray, N. J., and Rebelo, L-M.: Global Mangrove Extent Change 1996 - 2020: Global Mangrove Watch Version 3.0, *Remote Sensing*, 14, 3657, <https://doi.org/10.3390/rs14153657>, 2022.
- Cai, W. J.: Estuarine and coastal ocean carbon paradox: CO₂ sinks or sites of terrestrial carbon incineration?, *Annu. Rev. Marine Sci.*, 3, 123-145, 2011.
- 585 Canadell, J., Ciais, P., Sabine, C., and Joos, F. (Eds.): *Regional Carbon Cycle Assessment and Processes (RECCAP)*, Biogeosciences, special issue107, 2012.
- Castelão, R. M., and Möller, O. O.: A Modeling Study of Patos Lagoon (Brazil) Flow Response to Idealized Wind and River Discharge: Dynamical Analysis, *Brazilian Journal of Oceanography*, 54(1), 1-17, 2006.
- 590 Cataudella, S., Crosetti, D., and Massa, F.: Mediterranean coastal lagoons: sustainable management and interactions among aquaculture, capture fisheries and the environment *Studies and Reviews. General Fisheries Commission for the Mediterranean. No 95*, edited by Cataudella, S., Crosetti, D., and Massa, F., Rome, FAO, 278 pp, 2015.
- CDELM Centro de Documentación “Ecosistemas Litorales Mexicanos”: estuarine online database *http://izt.uam.mx/ocl/index2.html*, last accessed October, 4th 2022, 2003.
- 595 Chauvaud, L., Jean, F., Ragueneau, O., and Thouzeau, G.: Long-term variation of the Bay of Brest ecosystem: benthic-pelagic coupling revisited, *Mar. Ecol. Prog. Ser.*, 200, 35-48, 2000.
- Chen, C. T. A., and Borges, A. V.: Reconciling opposing views on carbon cycling in the coastal ocean: continental shelves as sinks and near-shore ecosystems as sources of atmospheric CO₂, *Deep-Sea Res. Pt. II*, 56, 578-590, 600 2009.
- Chen, C.-T. A., Huang, T.-H., Chen, Y.-C., Bai, Y., He, X., and Kang, Y.: Air–sea exchanges of CO₂ in the world’s coastal seas, *Biogeosciences*, 10, 6509-6544, <https://doi.org/10.5194/bg-10-6509-2013>, 2013.
- Chuang, P.-C., Young, M. B., Dale, A. W., Miller, L. G., Herrera-Silveira, J. A., and Paytan, A.: Methane fluxes from tropical coastal lagoons surrounded by mangroves, Yucatán, Mexico: methane fluxes from coastal lagoons, 605 *J. Geophys. Res. Biogeosci.*, 122(5), 1156-1174, doi:10.1002/2017JG003761, 2017.
- Chubarenko, B., and Margoński, P.: The Vistula Lagoon, in: *Ecology of Baltic Coastal Waters. Ecological Studies*, vol 197, edited by Schiewer, U., Springer, Berlin, Heidelberg, doi:10.1007/978-3-540-73524-3_8, 2008.
- Ciais, P., Bastos, A., Chevallier, F., Lauerwald, R., Poulter, B., Canadell, J. G., Hugelius, G., Jackson, R. B., Jain, A., Jones, M., Kondo, M., Lujikx, I. T., Patra, P. K., Peters, W., Pongratz, J., Petrescu, A. M. R., Piao, S., Qiu, 610 C., Von Randow, C., Regnier, P., Saunois, M., Scholes, R., Shvidenko, A., Tian, H., Yang, H., Wang, X., and Zheng, B.: Definitions and methods to estimate regional land carbon fluxes for the second phase of the Regional Carbon Cycle Assessment and Processes Project (RECCAP-2), *Geosci. Model Dev.*, 15, 1289-1316, doi:10.5194/gmd-15-1289-2022, 2022.
- Ciais, P., Yao, Y., Gasser, T., Baccini, A., Wang, Y., Lauerwald, R., Peng, S., Bastos, A., Li, W., Raymond, P. 615 A., Canadell, J. G., Peters, G. P., Andres, R. J., Chang, J., Yue, C., Dolman, A. J., Haverd, V., Hartmann, J., Laruelle, G., Konings, A. G., King, A. W., Liu, Y., Luysaert, S., Maignan, F., Patra, P. K., Peregon, A., Regnier,

- P., Pongratz, J., Poulter, B., Shvidenko, A., Valentini, R., Wang, R., Broquet, G., Yin, Y., Zscheischler, J., Guenet, B., Goll, D. S., Ballantyne, A.-P., Yang, H., Qiu, C., and Zhu, D.: Empirical estimates of regional carbon budgets imply reduced global soil heterotrophic respiration, *Natl. Sci. Rev.*, 8(2), nwaal45, doi:10.1093/nsr/nwaa145, 620 2020.
- Cloern, J. E., Foster, S. Q., and Kleckner, A. E.: Phytoplankton primary production in the world's estuarine-coastal ecosystems, *Biogeosciences*, 11, 2477-2501, doi:10.5194/bg-11-2477-2014, 2014.
- Cole, J. J., Prairie, Y. T., Caraco, N. F., McDowell, W. H., Tranvik, L. J., Striegl, R. G., Duarte, C. M., Kortelainen, P., Downing, J. A., Middelburg, J. J., and Melack, J.: Plumbing the global carbon cycle: Integrating inland waters into the terrestrial carbon budget, *Ecosystems*, 10, 171-184, 2007. 625
- Coynel, A., Gorse, L., Curti, C., Schafer, J., Grosbois, C., Morelli, G., Ducassou, E., Blanc, G., Maillet, G. M., and Mojtahib, M.: Spatial distribution of trace elements in the surface sediments of a major European estuary (Loire Estuary, France): Source identification and evaluation of anthropogenic contribution, *Journal of Sea Research*, 118, 77-91, doi:10.1016/j.seares.2016.08.005, 2016.
- 630 Crossland, C. J., Kremer, H. H., Lindeboom, H. J., Marshall Crossland, J. I., and LeTissier, M. D. A.: Coastal Fluxes in the Anthropocene, *Global Change – The IGBP Series*, Berlin, Heidelberg, Springer, 2005.
- De la Paz, M., Gómez-Parra, A., and Fojja, J.M.: Inorganic carbon dynamic and air-water CO₂ exchange in the Guadalquivir Estuary (SW Iberian Peninsula), *Journal of Marine Systems*, 68, 265-277, 2007.
- DEFRA: Department for Environment, Food and Rural Affairs: The estuary guide, <http://www.estuary-guide.net/>, 635 Accessed 18 Feb 2009, 2008.
- Digby, M. J., Saenger, P., Whelan, M. B., McConchie, D., Eyre, B., Holmes, N., and Bucher, D.: A physical classification of Australian Estuaries. Report prepared for the urban water research association of Australia by the centre for coastal management. Lismore: Southern Cross University, 1998.
- Dinauer, A.: Inorganic carbon dynamics in the Estuary and Gulf of St. Lawrence: A source or sink of atmospheric carbon dioxide and factors that control the spatial variability in gas exchange. MSc thesis, McGill University (Canada) ProQuest Dissertations Publishing, 2017. 640
- Dinauer, A., and Mucci, A.: Spatial variability in surface-water pCO₂ and gas exchange in the world's largest semi-enclosed estuarine system: St. Lawrence Estuary (Canada), *Biogeosciences*, 14, 3221-3237, 2017.
- Dinnel, S. P., Schroeder, W. W., and Wiseman, W. J. Jr.: Estuarine-shelf exchange using Landsat images of discharge plumes, *Journal of Coastal Research*, 6(4), 789-799, 1990. 645
- Downing, J. A., Prairie, Y. T., Cole, J. J., Duarte, C. M., Tranvik, L. J., Striegl, R. G., McDowell, W. H., Kortelainen, P., Caraco, N. F., Melack, J. M., and Middelburg, J. J.: The global abundance and size distribution of lakes, ponds, and impoundments, *Limnol. Oceanogr.*, 51, 2388-2397, doi:10.4319/lo.2006.51.5.2388, 2006.
- Dürr, H. H., Laruelle, G. G., van Kempen, C. M., Slomp, C. P., Meybeck, M., and Middelkoop, H.: Worldwide 650 Typology of Nearshore Coastal Systems: Defining the Estuarine Filter of River Inputs to the Oceans, *Estuar. Coast.*, 34, 441-458, doi:10.1007/s12237-011-9381-y, 2011.
- Elliott, M., and McLusky, D. S.: The need for definitions in understanding estuaries, *Estuarine, Coastal and Shelf Science*, 55, 815-827, 2002.
- Engle, V. D., Kurtz, J. C., Smith, L. M., Chancy, C., and Bourgeois, P.: A classification of U.S. estuaries based 655 on physical and hydrologic attributes, *Environ. Monit. Assess.*, 129, 397-412, 2007.

- Ericson, J. P., Vorosmarty, C. J., Dingman, S. L., Ward, L. G. and Meybeck, M.: Effective sea-level rise and deltas: Causes of change and human dimension implications, *Global Planetary Change*, 50, 63-82, 2005.
- Leal Filho, W., Nagy, G. J., Martinho, F., Saroar, M., Erache, M. G., Primo, A. L., Pardal, M. A., and Li, C.: Influences of Climate Change and Variability on Estuarine Ecosystems: An Impact Study in Selected European, South American and Asian Countries, *Int. J. Environ. Res. Public Health*, 19, 585, doi:10.3390/ijerph19010585, 2022.
- Friedlingstein, P., O'Sullivan, M., Jones, M. W., Andrew, R. M., Gregor, L., Hauck, J., Le Quéré, C., Luijckx, I. T., Olsen, A., Peters, G. P., Peters, W., Pongratz, J., Schwingshackl, C., Sitch, S., Canadell, J. G., Ciais, P., Jackson, R. B., Alin, S. R., Alkama, R., Arneeth, A., Arora, V. K., Bates, N. R., Becker, M., Bellouin, N., Bittig, H. C., Bopp, L., Chevallier, F., Chini, L. P., Cronin, M., Evans, W., Falk, S., Feely, R. A., Gasser, T., Gehlen, M., Gkritzalis, T., Gloege, L., Grassi, G., Gruber, N., Gürses, Ö., Harris, I., Hefner, M., Houghton, R. A., Hurtt, G. C., Iida, Y., Ilyina, T., Jain, A. K., Jersild, A., Kadono, K., Kato, E., Kennedy, D., Klein Goldewijk, K., Knauer, J., Korsbakken, J. I., Landschützer, P., Lefèvre, N., Lindsay, K., Liu, J., Liu, Z., Marland, G., Mayot, N., McGrath, M. J., Metzl, N., Monacchi, N. M., Munro, D. R., Nakaoka, S.-I., Niwa, Y., O'Brien, K., Ono, T., Palmer, P. I., Pan, N., Pierrot, D., Pockock, K., Poulter, B., Resplandy, L., Robertson, E., Rödenbeck, C., Rodriguez, C., Rosan, T. M., Schwinger, J., Séférian, R., Shutler, J. D., Skjelvan, I., Steinhoff, T., Sun, Q., Sutton, A. J., Sweeney, C., Takao, S., Tanhua, T., Tans, P. P., Tian, X., Tian, H., Tilbrook, B., Tsujino, H., Tubiello, F., van der Werf, G. R., Walker, A. P., Wanninkhof, R., Whitehead, C., Willstrand Wranne, A., Wright, R., Yuan, W., Yue, C., Yue, X., Zaehle, S., Zeng, J., and Zheng, B.: Global Carbon Budget 2022, *Earth Syst. Sci. Data*, 14, 4811-4900, <https://doi.org/10.5194/essd-14-4811-2022>, 2022.
- Gattuso, J.-P., Frankignoulle, M., and Wollast, R.: Carbon and carbonate metabolism in coastal aquatic ecosystems, *Annu. Rev. Ecol. Syst.*, 29, 405-433, 1998.
- Grelowski, A., Pastuszek, M., Sitek, S., and Witek, Z.: Budget calculations of nitrogen, phosphorus and BOD passing through the Oder estuary, *Journal of Marine Systems*, 25, 221-237, doi:10.1016/S0924-7963(00)00017-8, 2000.
- Guiral, D., and Ferhi, A.: Hydrodynamics of Ebrié Lagoon as revealed by a chemical and isotopic study, *Hydrobiologia*, 245 (2), 65-74, doi:10.1007/BF00764766, 1992.
- Harris, P., Muelbert, J., Muniz, P., Yin, K., Ahmed, K., Folorunsho, F., Caso, M., Vale, C. C., Machiwa, J., Ferreira, B., Bernal, P., and Rice, J.: Estuaries and Deltas, in: United Nations World Ocean Assessment, edited by Inniss, L., Simcock, A., Ajawin, A. Y., Alcala, A. C., Bernal, P., Calumpang, H. P., Araghi, P. E., Green, S. O., Kunio, K., Kohata, O. K., Marschoff, E., Martin, G., Ferreira, B. P., Park, C., Payet, R. A., Rice, J., Rosenberg, A., Ruwa, R., Tuhumwire, J. T., Gaever, S. V., Wang, J., and Węśławski, J. M., Cambridge University Press, Cambridge, 2016.
- Herdendorf, C. E.: Large Lakes of the World, *Journal of Great Lakes Research*, 8(3), 379-412, 1982.
- Jung, N. W., Lee, G.-H., Jung, Y., Figueroa, S. M., Lagamayo, K. D., Jo, T.-C., and Chang, J.: MorphEst: An Automated Toolbox for Measuring Estuarine Planform Geometry from Remotely Sensed Imagery and Its Application to the South Korean Coast, *Remote Sens.*, 13, 330, <https://doi.org/10.3390/rs13020330>, 2021.
- Hume, T., Gerbeaux, P., Hart, D., Kettles, H., and Neale, D.: A classification of New Zealand's coastal hydrosystems, 120, Hamilton: Ministry of the Environment, 2016.

- 695 Kang, Y., Pan, D., Bai, Y., He, X., Chen, X., Chen, C.-T. A., and Wang, D.: Areas of the global major river plumes, *Acta Oceanologica Sinica*, 32(1), 79-88, doi: 10.1007/s13131-013-0269-5, 2013.
- Kennish, M.: Environmental threats and environmental future of estuaries, *Environmental Conservation*, 29(1), 78-107, doi:10.1017/S0376892902000061, 2002.
- Laruelle, G. G.: Quantifying nutrient cycling and retention in coastal waters at the global scale, Ph.D. dissertation, 700 Utrecht University, 2009.
- Laruelle, G. G., Regnier, P., Ragueneau, O., Kempa, M., Moriceau, B., Ni Longphuir, S., Leynaert, A., Thouzeau, G., and Chauvaud, L.: Benthic-pelagic coupling and the seasonal silica cycle in the Bay of Brest (France): new insights from a coupled physical-biological model, *Mar. Ecol.-Prog. Ser.*, 385, 15-32, 2009.
- Laruelle, G. G., Roubex, V., Sferratore, A., Brodherr, B., Ciuffa, D., Conley, D. J., Dürr, H. H., Garnier, J., 705 Lancelot, C., Le Thi Phuong, Q., Meunier, J.-D., Meybeck, M., Michalopoulos, P., Moriceau, B., Ní Longphuir, S., Loucaides, S., Pa push, L., Presti, M., Ragueneau, O., Regnier, P. A. G., Saccone, L., Slomp, C. P., Spiteri, C., and Van Cappellen, P.: Anthropogenic perturbations of the silicon cycle at the global scale: Key role of the land-ocean transition, *Global Biogeochem. Cy.*, 23, doi:10.1029/2008GB003267, 2009.
- Laruelle, G. G., Dürr, H. H., Slomp, C. P., and Borges, A. V.: Evaluation of sinks and sources of CO₂ in the 710 global coastal ocean using a spatially-explicit typology of estuaries and continental shelves, *Geophys. Res. Lett.*, 37, L15607, doi:10.1029/2010GL043691, 2010.
- Laruelle, G. G., Dürr, H. H., Lauerwald, R., Hartmann, J., Slomp, C. P., Goossens, N., and Regnier, P. A. G.: Global multi-scale segmentation of continental and coastal waters from the watersheds to the continental margins, *Hydrol. Earth Syst. Sci.*, 17, 2029-2051, doi:10.5194/hess-17-2029-2013, 2013.
- 715 Laruelle, G. G., Goossens, N., Arndt, S., Cai, W.-J., and Regnier, P.: Air-water CO₂ evasion from US East Coast estuaries, *Biogeosciences*, 14, 2441-2468, doi:10.5194/bg-14-2441-2017, 2017.
- Laruelle, G. G., Marescaux, A., Gendre, R. Le, Garnier, J., Rabouille, C., Thieu, V., and Lehrter, J. C.: Carbon Dynamics Along the Seine River Network: Insight from a Coupled Estuarine/River Modeling Approach, *Frontiers in Marine Science*, 6, 1-16, doi:10.3389/fmars.2019.00216, 2019.
- 720 Laval, B., Imberger, J. Y., and Findikakis, N.: Dynamics of a large tropical lake: Lake Maracaibo, *Aquatic Sciences*, 67(3), 337-349, 2005.
- Lehner, B., Verdin, K., and Jarvis, A.: New global hydrography derived from spaceborne elevation data, *Eos, Transactions American Geophysical Union*, 89(10), 93-94, 2008.
- Liu, K.-K., Atkinson, L., Quinones, R., and Talaue-McManus, L. (Eds.): Carbon and Nutrient Fluxes in 725 Continental Margins, *Global Change – The IGBP Series*, 3, Springer-Verlag Berlin Heidelberg, 2010
- Maavara, T., Lauerwald, R., Laruelle, G., Akbarzadeh, Z., Bouskill, N., Van Cappellen, P., and Regnier, P.: Nitrous oxide emissions from inland waters: Are IPCC estimates too high?, *Glob. Change Biol.*, 25, 473-488, doi:10.1111/gcb.14504, 2019.
- Mackenzie, F. T., Ver, L. M., Sabine, C., Lane, M., and Lerman, A.: C, N, P, S global biogeochemical cycles and 730 modeling of global change, in: *Interactions of C, N, P and S Biogeochemical Cycles and Global Change*, edited by: Wollast, R., Mackenzie, F. T., and Chou, L., 1-62, Springer-Verlag, 1993.
- Mackenzie, F. T., Ver, L. M., and Lerman, A.: Coupled biogeochemical cycles of carbon, nitrogen, phosphorus, and sulfur in the land-ocean-atmosphere system, in: *Asian Change in the Context of Global Change*, edited by: Galloway, J. N. and Melillo, J. M., Cambridge University Press, Cambridge, 42-100, 1998.

- 735 Mackenzie, F. T., De Carlo, E. H., and Lerman, A.: Coupled C, N, P, and O biogeochemical cycling at the land-ocean interface. In *Treatise on Estuarine and Coastal Science*, edited by: Middelburg, J. J. and Laane, R., Ch. 5.10, Elsevier, 2012.
- McCarthy, M. J., Otis, D. B., Mendez-Lazaro, P., and Muller-Karger, F. E.: Water quality drivers in 11 Gulf of Mexico estuaries, *Remote Sens (Basel)*, 10(2), 255, doi:10.3390/rs10020255, 2018.
- 740 Mantoura, R. E C., Martin, J.-M., and Wollast, R. (Eds.): *Ocean margin processes in global change*, Wiley, 1991.
- Massey, F. J.: "The Kolmogorov-Smirnov Test for Goodness of Fit.", *Journal of the American Statistical Association*, 46(253), 68-78, 1951.
- Mayorga, E., Seitzinger, S. P., Harrison, J. A., Dumont, E., Beusen, A. H. W., Bouwman, A. F., Fekete, B. M., Kroeze, C., and Van Drecht, G.: Global nutrient export from watersheds 2 (NEWS 2): model development and
745 implementation, *Environ Model Softw*, 25(7), 837-853, 2010.
- McKee, B. A., Aller, R. C., Allison, M. A., Bianchi, T. S., and Kineke, G. C.: Transport and transformation of dissolved and particulate materials on continental margins influenced by major rivers: Benthic boundary layer and seabed processes, *Continental Shelf Research*, 24, 899-926, 2004.
- McSweeney, S. L., Kennedy, D. M., Rutherford, I. D., and Stout, J. C.: Intermittently Closed/Open Lakes and
750 Lagoons: Their global distribution and boundary conditions, *Geomorphology*, 292, 142-152, 2017.
- Meybeck, M., Dürr, H. H., and Vörosmary, C. J.: Global coastal segmentation and its river catchment contributors: A new look at land-ocean linkage, *Global Biogeochem. Cy.*, 20, GB1S90, doi:10.1029/2005GB002540, 2006.
- Murray, N. J., Phinn, S. R., DeWitt, M., Ferrari, R., Johnston, R., Lyons, M. B., Clinton, N., Thau, D., and Fuller,
755 R. A.: The global distribution and trajectory of tidal flats, *Nature*, 565, 222-225, <https://doi.org/10.1038/s41586-018-0805-8>, 2018.
- Murray, N. J., Worthington, T. A., Bunting, P., Duce, S., Hagger, V., Lovelock, C. E., Lucas, R., Saunders, M. I., Sheaves, M., Spalding, M., Waltham, N. J., and Lyons, M. B.: High-resolution mapping of losses and gains of Earth's tidal wetlands, *Science*, 376(6594), 744-749, doi:10.1126/science.abm9583, 2022.
- 760 Nedwell, D. B., Dong, L. F., Sage, A., and Underwood, G. J. C.: Variations of the nutrients loads to the mainland UK estuaries: correlation with catchment areas, urbanisation and coastal eutrophication, *Estuar. Coast. Shelf Sci.*, 54, 951-970, 2002.
- Nixon, S. W., J. W. Ammerman, L. P. Atkinson, V. M. Berounsky, G. Billen, W. C. Boicourt, W. R. Boynton, T. M. Church, D. M. Ditoro, R. Elmgren, J. H. Garber, A. E. Giblin, R. A. Jahnke, N. J. P. Owens, M. E. Q. Pilson,
765 and Seitzinger, S. P.: The fate of nitrogen and phosphorus at the land-sea margin of the North Atlantic Ocean, *Biogeochemistry*, 3, 141-180, 1996.
- Ortiz-Lozano, L., Granados-Barba, A., Solís-Weiss, V., and García-Salgado, M. A.: Environmental evaluation and development problems of the Mexican Coastal Zone, *Ocean & Coastal Management*, 48, 161-176, doi:10.1016/j.ocecoaman.2005.03.001, 2005.
- 770 Pagano, M., Kouassi, E., Arfi, R., Bouvy, M. and SaintJean, L.: In situ spawning rate of the Calanoid Copepod *Acartia clausi* in a tropical lagoon (Ebrié, Côte d'Ivoire): Diel variations and effects of environmental factors, *Zoological Studies*, 43(2), 244-254, 2004.
- Pritchard, D. W.: What is an estuary: physical viewpoint, in: *Estuaries*, AAAS, Washington DC, 3-5, Pub. 83, 1967.

- 775 Quasim, S. Z.: Production in some tropical environments, in *Marine Production Mechanics*, edited by Dunbar, M. J., Cambridge Univ. Press, London, 31-70, 1979.
- Rabouille, C., Mackenzie, F. T., and Ver, L. M.: Influence of the human perturbation on carbon, nitrogen, and oxygen biogeochemical cycles in the global coastal ocean, *Geochim. Cosmochim. Ac.*, 65, 3615-3641, 2001.
- Regnier, P., Friedlingstein, P., Ciais, P., Mackenzie, F. T., Gruber, N., Janssens, I., Laruelle, G. G., Lauerwald, R., Luysaert, S., Andersson, A. J., Arndt, S., Arnosti, C., Borges, A. V., Dale, A. W., Gallego-Sala, A., Godd ris, Y., Goossens, N., Hartmann, J., Heinze, C., Ilyina, T., Joos, F., LaRowe, D. E., Leifeld, J., Meysman, F. J. R., Munhoven, G., Raymond, P. A., Spahni, R., Suntharalingam, P., and Thullner, M.: Anthropogenic perturbation of the land to ocean carbon flux, *Nat. Geosci.*, 6, 597-607, doi:10.1038/NGEO1830, 2013a.
- 780 Regnier, P., Arndt, S., Goossens, N., Volta, C., Laruelle, G. G., Lauerwald, R., and Hartmann, J.: Modelling Estuarine Biogeochemical Dynamics: From the Local to the Global Scale, *Aquat. Geochem.*, 19, 591-626, doi:10.1007/s10498-013-9218-3, 2013b.
- 785 Regnier, P., Resplandy, L., Najjar, R.G., and Ciais, P.: The land-to-ocean loops of the global carbon cycle, *Nature* 603, 401-410, doi:10.1038/s41586-021-04339-9, 2022.
- Reinhart, V., Hoffmann, P., Rechid, D., B hner, J., and Bechtel, B.: High-resolution land use and land cover dataset for regional climate modelling: a plant functional type map for Europe 2015, *Earth Syst. Sci. Data*, 14, 1735-1794, doi:10.5194/essd-14-1735-2022, 2022.
- 790 Rosentreter, J. A., Laruelle, G. G., Bange, H. W., Bianchi, T. S., Busecke, J. J. M., Cai, W.-J., Eyre, B. D., Forbrich, I., Kwon, E. Y., Maavara, T., Moosdorf, N., Najjar, R. G., Sarma, V. V. S. S., Van Dam, B., and Regnier, P.: Coastal vegetation and estuaries collectively reduce global warming, submitted to *Nature Climate Change*
- 795 Sagar, B. S. D.: Universal scaling laws in surface water bodies and their zones of influence, *Water Resour. Res.*, 43, W02416, doi:10.1029/2006WR005075, 2007.
- Santoro, M., Cartus, O., Carvalhais, N., Rozendaal, D. M. A., Avitabile, V., Araza, A., de Bruin, S., Herold, M., Quegan, S., Rodr guez-Veiga, P., Balzter, H., Carreiras, J., Schepaschenko, D., Korets, M., Shimada, M., Itoh, T., Moreno Mart nez,  ., Cavlovic, J., Cazzolla Gatti, R., da Concei o Bispo, P., Dewnath, N., Labri re, N., Liang, J., Lindsell, J., Mitchard, E. T. A., Morel, A., Pacheco Pascagaza, A. M., Ryan, C. M., Slik, F., Vaglio Laurin, G., Verbeeck, H., Wijaya, A., and Willcock, S.: The global forest above-ground biomass pool for 2010 estimated from high-resolution satellite observations, *Earth Syst. Sci. Data*, 13, 3927-3950, i.org/10.5194/essd-13-3927-2021, 2021.
- 800 Saunois, M., Stavert, A. R., Poulter, B., Bousquet, P., Canadell, J. G., Jackson, R. B., Raymond, P. A., Dlugokencky, E. J., Houweling, S., Patra, P. K., Ciais, P., Arora, V. K., Bastviken, D., Bergamaschi, P., Blake, D. R., Brailsford, G., Bruhwiler, L., Carlson, K. M., Carrol, M., Castaldi, S., Chandra, N., Crevoisier, C., Crill, P. M., Covey, K., Curry, C. L., Etiope, G., Frankenberg, C., Gedney, N., Hegglin, M. I., H glund-Isaksson, L., Hugelius, G., Ishizawa, M., Ito, A., Janssens-Maenhout, G., Jensen, K. M., Joos, F., Kleinen, T., Krummel, P. B., Langenfelds, R. L., Laruelle, G. G., Liu, L., Machida, T., Maksyutov, S., McDonald, K. C., McNorton, J., Miller, P. A., Melton, J. R., Morino, I., M ller, J., Murgu a-Flores, F., Naik, V., Niwa, Y., Noce, S., O'Doherty, S., Parker, R. J., Peng, C., Peng, S., Peters, G. P., Prigent, C., Prinn, R., Ramonet, M., Regnier, P., Riley, W. J., Rosentreter, J. A., Segers, A., Simpson, I. J., Shi, H., Smith, S. J., Steele, L. P., Thornton, B. F., Tian, H., Tohjima, Y., Tubiello, F. N., Tsuruta, A., Viovy, N., Voulgarakis, A., Weber, T. S., van Weele, M., van der Werf, G. R., Weiss, R. F., Worthy, D., Wunch, D., Yin, Y., Yoshida, Y., Zhang, W., Zhang, Z., Zhao, Y., Zheng, B., Zhu, Q., Zhu, Q., and

- 815 Zhuang, Q.: The Global Methane Budget 2000–2017, *Earth Syst. Sci. Data*, 12, 1561–1623, [i.org/10.5194/essd-12-1561-2020](https://doi.org/10.5194/essd-12-1561-2020), 2020.
- Savenije, H.: *Salinity and Tides in Alluvial Estuaries*, Elsevier: Amsterdam, The Netherlands, 2005.
- Savenije, H. H. G. (Ed.): *Salinity and Tides in Alluvial Estuaries*, 2nd Edn., available at: <https://salinityandtides.com/> (last access: 8 March 2015), 2012.
- 820 Sayre, R., Noble, S., Hamann, S., Smith, R., Wright, D., Breyer, S., Butler, K., Van Graafeiland, K., Frye, C., Karagulle, D., Hopkins, D., Stephens, D., Kelly, K., Basher, Z., Burton, D., Cress, J., Atkins, K., Van Sistine, D. P., Friesen, B., Allee, R., Allen, T., Aniello, P., Asaad, I., Costello, M. J., Goodin, K., Harris, P., Kavanaugh, M., Lillis, H., Manca, E., Muller-Karger, F., Nyberg, B., Parsons, R., Saarinen, J., Steiner, J., and Reed, A.: A new 30 meter resolution global shoreline vector and associated global islands database for the development of
- 825 standardized ecological coastal units, *J. Oper. Oceanogr.*, 12, S47-S56, <https://doi.org/10.1080/1755876x.2018.1529714>, 2018.
- Schartup, A. T., Balcom, P. H., Soerensen, A. L., Gosnell, K. J., Calder, R. S. D., Mason, R. P., and Sunderland, E. M.: Freshwater discharges drive high levels of methylmercury in Arctic marine biota, *PNAS*, 112(38), 11789-11794, 2015.
- 830 Seitzinger, S. P., Harrison, J. A., Dumont, E., Beusen, A. H. W., and Bouwman, A. F.: Sources and delivery of carbon, nitrogen, and phosphorus to the coastal zone: An overview of Global Nutrient Export from Watersheds (NEWS) models and their application, *Global Biogeochem. Cycles*, 19, GB4S01, [doi:10.1029/2005GB002606](https://doi.org/10.1029/2005GB002606), 2005.
- Sfriso, A., Buosi, A., Mistri, M., Munari, C., Franzoi, P., and Sfriso, A. A.: Long-term changes of the trophic
- 835 status in transitional ecosystems of the northern Adriatic Sea, key parameters and future expectations: The lagoon of Venice as a study case, *Nature Conservation*, 34, 193-215, [doi:10.3897/natureconservation.34.30473](https://doi.org/10.3897/natureconservation.34.30473), 2019.
- SMHI: Swedish Oceanographic Data Center, <http://www.smhi.se/cmp/jsp/polopoly.jsp?d=5431&l=sv>, Accessed 1 May 2009, 2009.
- Solidoro, C., Pastres, R., and Cossarini, G.: Nitrogen and plankton dynamics in the lagoon of Venice, *Ecol. Model.*
- 840 184, 103-123, [i.org/10.1016/j.ecolmodel.2004.11.009](https://doi.org/10.1016/j.ecolmodel.2004.11.009), 2005
- Sørnes, T. A., and Aksnes, D.L.: Concurrent temporal patterns in light absorbance and fish abundance, *Marine Ecology Progress Series* 325: 181-186, 2006.
- Stankevicius, A., (ed.): *Annual report of scientific work, Klaipėda, Center of Marine Research: 1-90*, 1995.
- Syvitski, J. P. M., Burrell, D. C., and Skei, J. M.: *Fjords: processes and products*. New York: Springer, 1987.
- 845 Tian, H., Xu, R., Canadell, J. G., Thompson, R. L., Winiwarter, W., Suntharalingam, P., Davidson, E. A., Ciais, P., Jackson, R. B., Janssens-Maenhout, G., Prather, M. J., Regnier, P., Pan, N., Pan, S., Peters, G. P., Shi, H., Tubiello, F. N., Zaehle, S., Zhou, F., Arneth, A., Battaglia, G., Berthet, S., Bopp, L., Bouwman, A. F., Buitenhuis, E. T., Chang, J., Chipperfield, M. P., Dangal, S. R. S., Dlugokencky, E., Elkins, J. W., Eyre, B. D., Fu, B., Hall, B. D., Ito, A., Joos, F., Krummel, P. B., Landolfi, A., Laruelle, G. G., Lauerwald, R., Li, W., Lienert, S., Maavara,
- 850 T., Macleod, M., Millet, D. B., Olin, S., Patra, P. K., Prinn, R. G., Raymond, P. A., Ruiz, D. J., van der Werf, G. R., Vuichard, N., Wang, J., Weiss, R. F., Wells, K. C., Wilson, C., Yang, J., and Yao, Y.: A comprehensive quantification of global nitrous oxide sources and sinks, *Nature*, 586, 248-256, [doi:10.1038/s41586-020-2780-0](https://doi.org/10.1038/s41586-020-2780-0), 2020.

- Tootchi, A., Jost, A., and Ducharne, A.: Multi-source global wetland maps combining surface water imagery and groundwater constraints, *Earth Syst. Sci. Data*, 11, 189–220, doi:10.5194/essd-11-189-2019, 2019.
- Schwartz, M.L.: *Encyclopedia of coastal science*. Dordrecht: Springer, 2005.
- UNESCO-IOC: African Oceans and Coasts, in *IOC Information Document*, 1255 edited by Odido, M., and Mazzilli S., UNESCO Regional Bureau for Science and Technology in Africa, Kenya, 2009.
- Upstill-Goddard, R. C., and Barnes, J.: Methane emissions from UK estuaries: re-evaluating the estuarine source of tropospheric methane from Europe, *Mar. Chem.*, 180, 14-23, <https://doi.org/10.1016/j.marchem.2016.01.010>, 2016.
- USEPA: Ecological condition of estuaries in the Gulf of Mexico, EPA 620-R-98-004, U.S. Environmental Protection Agency, Office of Research and Development, National Health and Environmental Effects Research Laboratory, Gulf Ecology Division, Gulf Breeze, Florida. 80 pp, 1999.
- USGS, United States Geological Survey: NAWQA Apalachicola River Basin Study, <http://usgs.gov/nawqa/index.html>, Last access October 5th, 2022, 2022.
- Vanderborght, J. P., Wollast, R., Loijens, M., and Regnier, P.: Application of a transport-reaction model to the estimation of biogas fluxes in the Scheldt estuary, *Biogeochemistry*, 59(1-2), 207-237. doi:10.1023/A:1015573131561, 2002.
- Van Niekerk, L., Adams, J. B, Bate, G. C., Forbes, A. T., Forbes, N. T., Huizinga, P., Lamberth, S. J., MacKay, C. F., Petersen, C., Taljaard, S., Weerts, S. P., Whitfield, A. K., and Wooldridge, T. H.: Country-wide assessment of estuary health: An approach for integrating pressures and ecosystem response in a data limited environment, *Estuarine, Coastal and Shelf Science*, 130, 239-251, 2013.
- Ver, L. M.: Global kinetic models of the coupled C, N, P, and S biogeochemical cycles: Implications for global environmental change, Ph.D. dissertation, University of Hawaii, 1998.
- Ver, L. M., Mackenzie, F. T., and Lerman, A.: Biogeochemical responses of the carbon cycle to natural and human perturbations: Past, present, and future, *Am. J. Sci.* 299, 762-801, 1999.
- Volta, C., Laruelle, G. G., and Regnier, P.: Regional carbon and CO₂ budgets of North Sea tidal estuaries, *Estuar. Coast. Shelf Sci.*, 176, 76-90, 2016.
- Wei, X., Garnier, J., Thieu, V., Passy, P., Le Gendre, R., Billen, G., Akopian, M., and Laruelle, G. G.: Nutrient transport and transformation in macrotidal estuaries of the French Atlantic coast: a modeling approach using the Carbon-Generic Estuarine Model, *Biogeosciences*, 19, 931-955, <https://doi.org/10.5194/bg-19-931-2022>, 2022.
- Wells, N. S., Maher, D. T., Erlar, D. V., Hipsey, M., Rosentreter, J. A., and Eyre, B. D.: Estuaries as Sources and Sinks of N₂O Across a Land Use Gradient in Subtropical Australia, *Global Biogeochem. Cycles*, 32, 877-894, doi:10.1029/2017GB005826, 2018.
- Wong, M. H., and Cheung, K. C.: China Estuarine Systems: Pearl River Estuary and Mirs Bay, in: *Estuarine Systems of the South China Sea Region: Carbon, Nitrogen and Phosphorus* edited by Smith, S.V., Dupra, V., Marshall Crossland, J. I., and Crossland, C. J., *LOCIZ Reports and Studies 14*, LOICZ, Texel, The Netherlands, 7-16, 2000.
- Woodland, R. J., Thomson, J. R., Mac Nally, R., Reich, P., Evrard, V., Wary, F. Y., Walker, J. P., and Cook, P. L. M.: Nitrogen loads explain primary productivity in estuaries at the ecosystem scale, *Limnol. Oceanol.*, 60(5), 1751-1762, <https://doi.org/10.1002/lno.10136>, 2015.

Woodwell, G. M., Rich, P. H., and Hall, C. A. S.: Carbon in estuaries, in: Carbon and the Biosphere, edited by Woodwell, G. M., and Pecan, E. V., U.S. Atomic Commission, Springfield, VA, pp. 221-240, 1973.

895

Table 1: List of estuarine systems for which several independent surface area estimates have been published (or calculated in the context of this study)

System	Type	km ²	reference	km ²	reference	km ²	reference
Bay of Brest	Tidal	135	Laruelle et al., 2009	180	Chauvaud et al., 2000	161	This study
Chesapeake Bay	Tidal	10,073	Dürr et al., 2011	11,542	Nixon et al., 1996	11,300	US Database
		10,421	Alder, 2003				
Delaware Bay	Tidal	1,980	Dürr et al., 2011	1,989	Nixon et al., 1996	2,700	US Database
		1,957	Alder, 2003				
Dvina	Tidal	288	Dürr et al., 2011	321	Alder, 2003	358	This study
Gambia	Tidal	611	Dürr et al., 2011	1,167	Alder, 2003	831	This study
Gironde	Tidal	604	Dürr et al., 2011	635	Audry et al., 2007	781	Wei et al., 2022
		650	Coynel et al., 2016	477	Alder, 2003		
Guadalquivir	Tidal	38	Dürr et al., 2011	48	Alder, 2003	39	de la Paz, 2007
Humber	Tidal	291	Dürr et al., 2011	303	Nedwell et al., 2002	220	Volta et al., 2016
		156	Alder, 2003				
Loire	Tidal	111	Dürr et al., 2011	151	Alder, 2003	185	Wei et al., 2022
		220	Coynel et al., 2016				
Mahi	Tidal	245	Dürr et al., 2011	258	Alder, 2003	316	This study
Mezen	Tidal	174	Dürr et al., 2011	157	Alder, 2003	162	Rimsky-Korsakov et al., 2018
Pearl River	Tidal	2,753	Dürr et al., 2011	1,993	This study	1,970	Wong and Cheung, 2000
		2,196	Alder, 2003				
Scheldt	Tidal	383	Dürr et al., 2011	277	Nixon et al., 1996	220	Volta et al., 2016
		337	Alder, 2003				
Seine	Tidal	143	Dürr et al., 2011	146	Laruelle et al., 2019	103	Alder, 2003
St Lawrence	Tidal	12,245	Dürr et al., 2011	12,820	Dinauer, 2017	12,781	Dinauer and Mucci, 2017
Yangtze	Tidal	2,432	Dürr et al., 2011	3,841	Alder, 2003	3,011	This study
Apalachicola Bay	Lagoon	813	Dürr et al., 2011	554	USGS, 2002	593	US database
Chelem Lagoon	Lagoon	13	Alder, 2003	14	Chuang et al., 2017	14	CDELM, 2003
Choctawhatchee	Lagoon	246	Dürr et al., 2011	344	Alder, 2003	340	US database
		334	USEPA, 1999				
Curonian Lagoon	Lagoon	1,602	Dürr et al., 2011	1,587	Alder, 2003	1,584	Stankevicius, 1995
Ebrie Lagoon	Lagoon	596	Alder, 2003	536	Pagano et al., 2004	566	Guiral and Ferhi, 1992
		560	UNESCO, 2009				
Galveston Bay	Lagoon	1,450	Alder, 2003	1,460	US database	1,550	Mc Carthy et al., 2018
Laguna de Terminos	Lagoon	1,660	Dürr et al., 2011	1,658	Alder, 2003	1,960	CDLEM, 2003
		1,700	Salles et al., 2002				
Maracaibo Lake	Lagoon	12,695	Dürr et al., 2011	13,210	Laval et al., 2005	12,882	This study
Mobile Bay	Lagoon	989	Dürr et al., 2011	1,064	Alder, 2003	1,059	Mc Carthy et al., 2018
		1,080	US database	958	Dinnel et al., 1990		
Oder Lagoon	Lagoon	844	Dürr et al., 2011	1,000	Grelowski et al., 2000	968	Patureij, 2018
Patos Lagoon	Lagoon	9,851	Dürr et al., 2011	10,000	Castelao and Moller, 2006	9,100	Patureij, 2018
		10,200	Alder, 2003				
Venice Lagoon	Lagoon	388	Dürr et al., 2011	500	Solidoro et al., 2005	432	Sfriso et al., 2019
Vistula Lagoon	Lagoon	740	Dürr et al., 2011	838	Patureij, 2018	838	Chubarenko and Margoński, 2008
Baker's fjord	Fjord	1,170	Dürr et al., 2011	1,300	Alder, 2003		
Lake Melville	Fjord	2984	Alder, 2003	3,069	Herdendorf, 1982	3,000	Schartup et al., 2015
		2,942	This study				
Sognefjord	Fjord	898	Dürr et al., 2011	950	Sørnes and Aksnes, 2006	955	This study
Trondheims Fjord	Fjord	1,503	Dürr et al., 2011	1,372	Alder, 2003	1,531	Thus study

Table 2: Calculated estuarine surface area per estuary type for each MARCATS. The relative uncertainties reported correspond to 2σ (95% confidence intervals).

MARCATS region		Deltas and tidal systems	Lagoons	Fjords	Total
Name	Number	km ²	km ²	km ²	km ²
North-eastern Pacific	1	1697 ± 1085	219 ± 124	13328 ± 2507	15244 ± 2735
California Current	2	2415 ± 861	6902 ± 1609	0	9317 ± 1825
Tropical Eastern Pacific	3	4365 ± 1610	1879 ± 415	0	6244 ± 1662
Peruvian Upwelling Current	4	85 ± 32	13 ± 7	0	98 ± 32
South America	5	3175 ± 1192	0	21988 ± 4113	25163 ± 4282
Brazilian Current	6	21877 ± 8009	16346 ± 3807	0	38223 ± 8868
Tropical Western Atlantic	7	32809 ± 11951	0	0	32809 ± 11951
Caribbean Sea	8	0	19692 ± 4309	0	19692 ± 4309
Gulf of Mexico	9	6213 ± 4723	33803 ± 8335	0	40016 ± 9580
Florida Upwelling	10	26412 ± 10452	16086 ± 3874	0	42498 ± 111147
Sea of Labrador	11	13148 ± 14328	0	11179 ± 2107	24327 ± 14482
Hudson Bay	12	2427 ± 1593	0	10276 ± 1937	12703 ± 2508
Canadian Archipelagos	13	6001 ± 3681	3863 ± 921	81816 ± 15524	91680 ± 15981
Northern Greenland	14	0	0	61135 ± 13861	61135 ± 13861
Southern Greenland	15	0	0	15910 ± 3246	15910 ± 3246
Norwegian Basin	16	0	0	16534 ± 3141	16534 ± 3141
North-eastern Atlantic	17	7721 ± 2985	727 ± 174	5050 ± 942	13498 ± 3135
Baltic Sea	18	195 ± 121	5567 ± 3120	2722 ± 1467	8484 ± 3450
Iberian Upwelling	19	2805 ± 1073	522 ± 288	0	3327 ± 1111
Mediterranean Sea	20	2051 ± 1292	9787 ± 89	0	11838 ± 1295
Black Sea	21	4155 ± 1544	2315 ± 536	0	6470 ± 1634
Moroccan Upwelling	22	8779 ± 3785	1223 ± 296	0	10002 ± 3797
Tropical Eastern Atlantic	23	8911 ± 3355	8812 ± 2152	0	17723 ± 3986
South-western Africa	24	208 ± 146	129 ± 73	0	337 ± 163
Agulhas Current	25	1984 ± 1340	1226 ± 298	0	3210 ± 1372
Tropical Western	26	685 ± 422	396 ± 223	0	1081 ± 477
Western Arabian Sea	27	443 ± 282	478 ± 270	0	921 ± 390
Red Sea	28	0	285 ± 68	0	285 ± 68
Persian Gulf	29	1395 ± 639	439 ± 97	0	1834 ± 646
Eastern Arabian Sea	30	5568 ± 2301	2196 ± 1219	0	7764 ± 2604
Bay of Bengal	31	18907 ± 7931	3101 ± 1711	0	22008 ± 8113
Tropical Eastern Indian	32	7864 ± 3039	1845 ± 418	0	9709 ± 3067
Leeuwin Current	33	20 ± 2	9773 ± 576	0	9793 ± 576
Southern Australia	34	3272 ± 126	3879 ± 84	0	7151 ± 151
Eastern Australian Current	35	1012 ± 50	2766 ± 37	0	3778 ± 62
New Zealand	36	5564 ± 105	693 ± 9	779 ± 18	7036 ± 106
Northern Australia	37	19946 ± 8037	1675 ± 384	0	21621 ± 8046
South East Asia	38	8747 ± 3606	1971 ± 460	0	10718 ± 3636
China Sea and Kuroshio	39	7189 ± 2537	1513 ± 844	0	8702 ± 2673
Sea of Japan	40	0	696 ± 399	0	696 ± 399
Sea of Okhotsk	41	4268 ± 3068	4592 ± 1100	0	8860 ± 3259
North-western Pacific	42	9020 ± 5789	3966 ± 902	948 ± 509	13934 ± 5881
Siberian Shelves	43	12728 ± 4612	8691 ± 1962	0	21419 ± 5012
Barents and Kara Seas	44	30895 ± 10745	1880 ± 443	17234 ± 3214	50009 ± 11224
Global total		294956±30780	179946±12056	258899±22328	733801 ± 39892

905 **Table 3: Estuarine surface area per type according to our calculations (this study) and extrapolated from Dürr et al. (2011) for each RECCAP region. Uncertainties are only available for our calculations and correspond to 2σ (95% confidence intervals).**

RECCAP			Deltas and tidal systems	Lagoons	Fjords	Total
Name	Number	Study	This study	This study	This study	This study
North	1	This study	67197 ± 19345	68044 ± 9627	193644 ± 21404	328885 ± 30415
		Dürr et al., 2011	47411	82257	298348	428016
South	2	This study	57946 ± 14436	31332 ± 5349	21988 ± 4113	111266 ± 15935
		Dürr et al., 2011	36011	21751	21265	79027
Europe	3	This study	14287 ± 3425	14452 ± 3154	24306 ± 3593	53044 ± 5886
		Dürr et al., 2011	37270	14063	67755	119088
Africa	4	This study	22494 ± 5252	14688 ± 2214	0	37182 ± 5699
		Dürr et al., 2011	28452	46052	10229	84733
Russia	5	This study	53548 ± 12788	20200 ± 2483	18182 ± 3254	91931 ± 13427
		Dürr et al., 2011	66493	25519	45265	137277
West Asia	6	This study	1395 ± 639	1070 ± 178	0	2465 ± 663
		Dürr et al., 2011	5265	0	0	5265
East Asia	7	This study	10421 ± 3353	2137 ± 924	0	12558 ± 3478
		Dürr et al., 2011	25715	13302	0	39017
South Asia	8	This study	22750 ± 7903	5421 ± 1228	0	28171 ± 7998
		Dürr et al., 2011	9913	11671	0	21585
Southeast	9	This study	19878 ± 6895	2542 ± 236	0	22420 ± 6899
		Dürr et al., 2011	67752	17284	0	85036
Australasia	10	This study	25041 ± 6344	20060 ± 780	779 ± 18	45880 ± 6392
		Dürr et al., 2011	37990	10784	2996	51770
Global total		This study	294956 ± 30780	179946 ± 12056	258899 ± 22328	733801 ± 39892
		Dürr et al., 2011	362272	242684	445859	1050815

Table 4: Geometric properties, simulated and observed salinity intrusion in several tidal estuaries. SA_S and AS_T correspond to the calculated surface area of the saline estuary and the surface area of the tidal estuary, respectively. H, B0, CL, LS, LT and Q represent geometric and hydrologic properties of each system and correspond to the tidal amplitude, the width at the mouth of the estuary, the estuarine convergence length, the length of the salt intrusion, the length of the tidal intrusion and the riverine freshwater discharge, respectively.

Estuary	H (m)	B0 (m)	CL (km)	LS (km)	LT (km)	Q (m ³ s ⁻¹)	SA S/SA T	Reference
Mae Klong	2	250	155	26	120	30	0.29	Savenjie, 2012
Limpopo	1.1	222	18	35	150	10	0.86	Savenjie, 2012
Lalang	2.7	371	96	65	200	50	0.56	Savenjie, 2012
Tha Chin	2.6	3600	87	60	120	5	0.67	Savenjie, 2012
Sinnamary	2.9	2100	39	70	150	10	0.85	Savenjie, 2012
Chao Phya	2.5	500	109	50	120	30	0.55	Savenjie, 2012
Ord	5.9	3200	22.1	50	65	1	0.95	Savenjie, 2012
Incomati	1.4	4500	42	70	100	20	0.89	Savenjie, 2012
Pungue	6.7	6512	21	40	120	10	0.85	Savenjie, 2012
Maputo	3.4	9000	16	90	100	20	0.99	Savenjie, 2012
Thames	4.3	7480	23	50	110	500	0.89	Savenjie, 2012
Corantijn	2.3	30,000	48	16	120	100	0.31	Savenjie, 2012
Gambia	1.2	9,687	121	300	500	2	0.93	Savenjie, 2012
Scheldt	3.7	15,207	28	110	200	90	0.98	Savenjie, 2012
Delaware	1.5	37,655	42	140	200	300	0.97	Savenjie, 2012
Seine	4.7	10,000	11	40	168	200	0.97	Laruelle et al., 2019
Loire	4.4	10,000	12	50	114	120	0.98	Wei et al., 2022

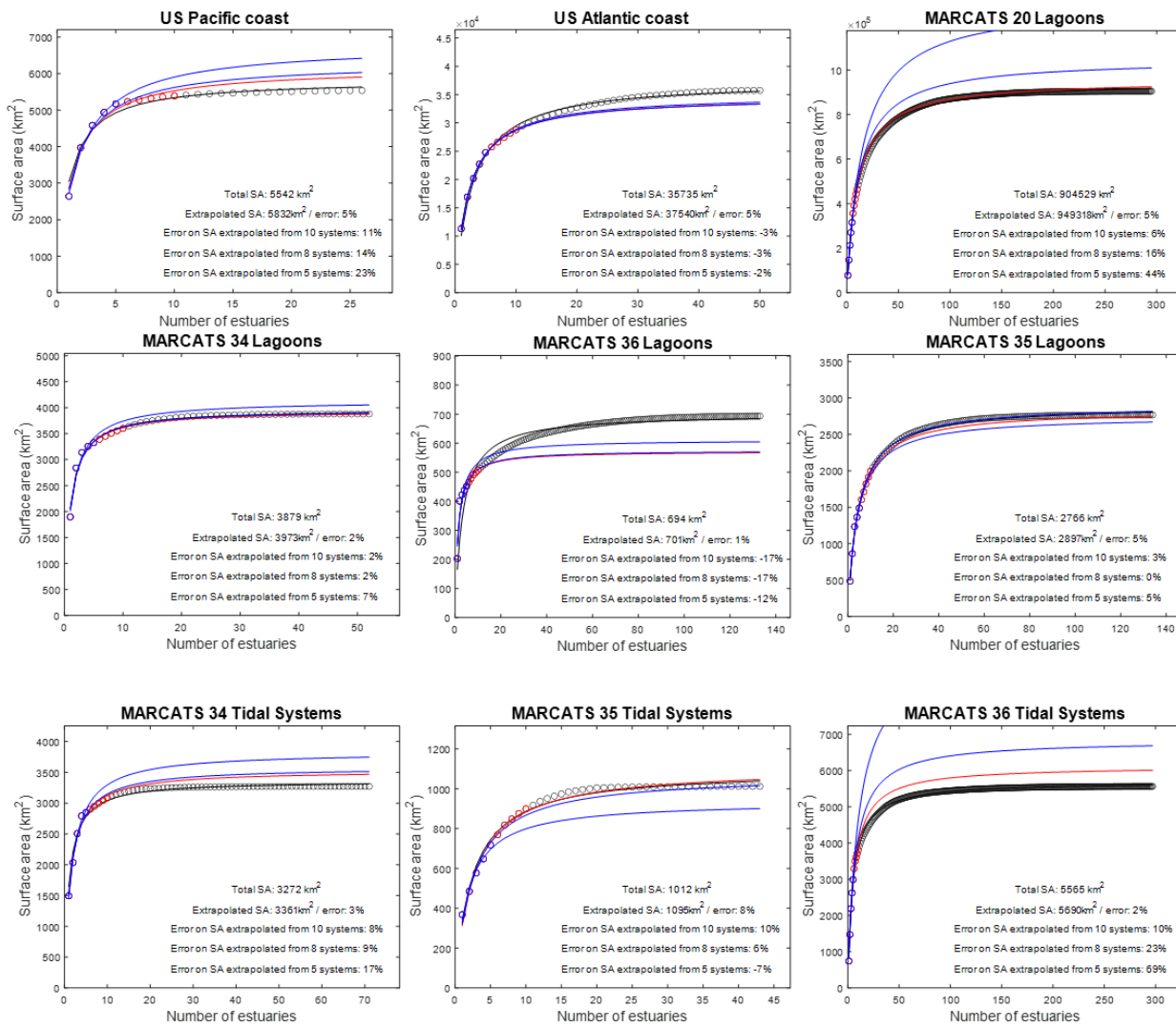


Figure 1: Evaluation of the term δ_M representing the uncertainty over our interpolation method for 9 MARCATS for which the total surface area is known through the application of our extrapolation method using the 5, 8 or 10 largest estuaries of the region only.

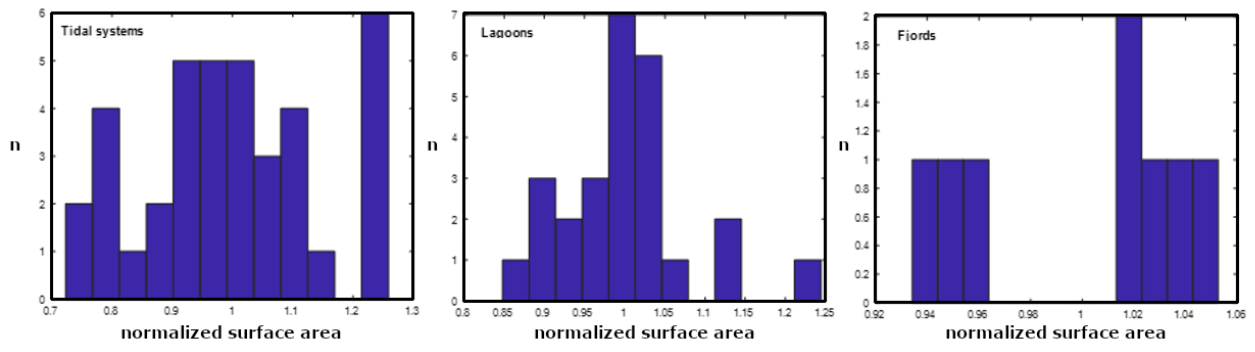
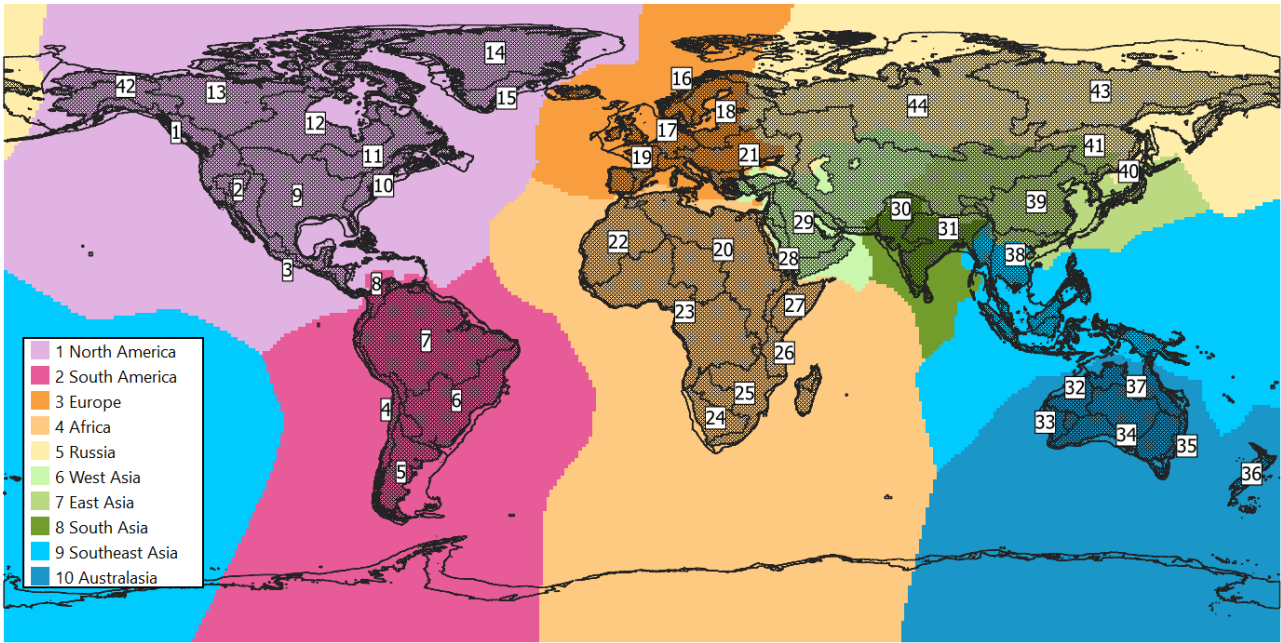


Figure 2: Histograms of the normalized surface areas of tidal systems and deltas (left), lagoons (middle) and fjords (right).



925 **Figure 3: Delineation of the RECCAP segmentation (in colours) and the MARACTS segmentation (shaded). The geographic extend of the MARCATS segmentation included all exorheic landmasses and continental shelves until the shelf break as defined in Laruelle et al., 2013.**

930

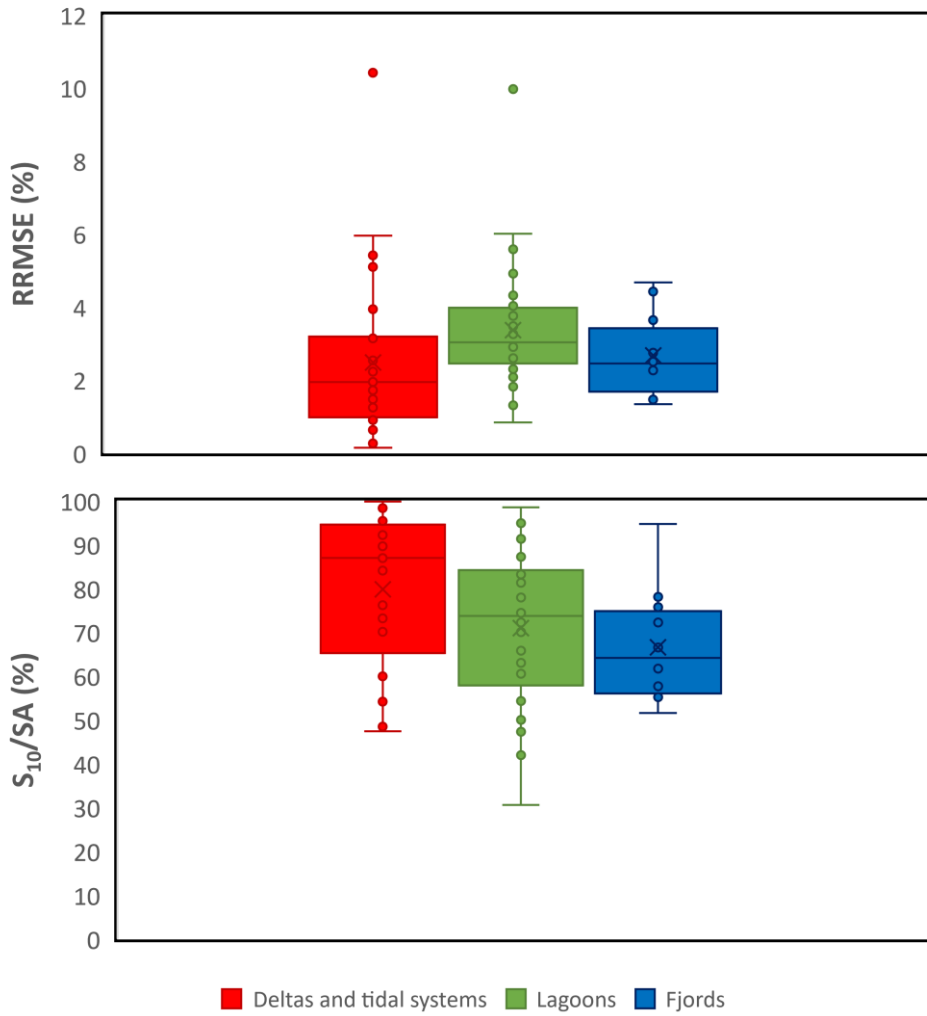
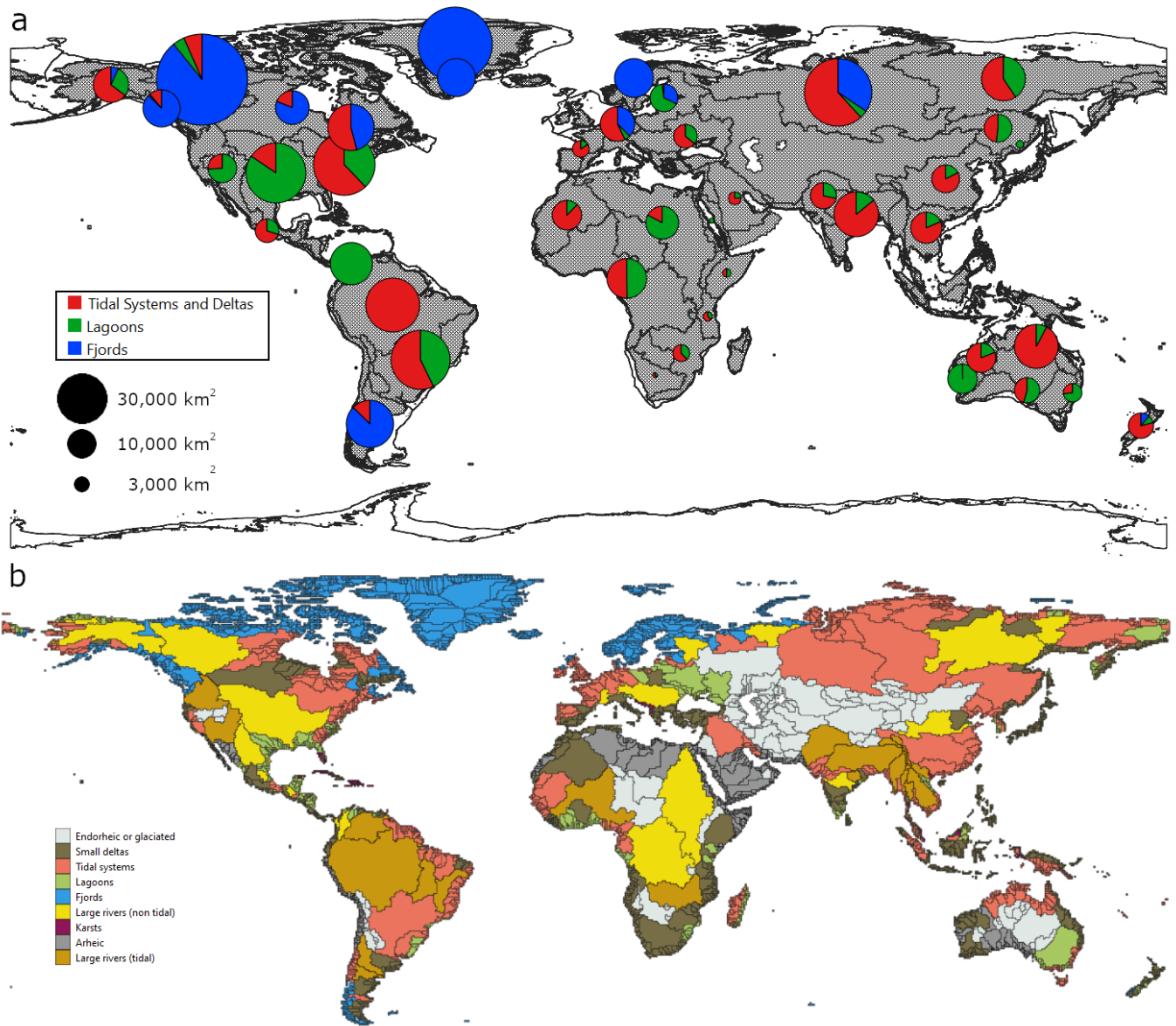


Figure 4: Distribution of the mean relative error (%) between the fitted and observed estuarine surface areas (RRMSE) within each MARCATS and estuarine type (top) and distribution of the proportion of the total estuarine surface area (SA) represented by the 10 largest systems (S₁₀) within a given MARCATS (bottom).



940 **Figure 5: Estuarine surface areas per MARCATS and per estuarine type expressed as pie-charts, which surface is proportional to the total estuarine surface area of the MARCATS (a) and global estuarine typology of Dürr et al. (2011) (b). For the sake of readability, the watersheds flowing into each estuary is coloured according to the type of the corresponding estuary on panel b.**